People's Democratic Republic of Algeria
Ministry of Higher Education and Scientific Research

University of August 20, 1955-Skikda

Faculty of Sciences

Department of Physics

N° : D02P2026M

Master's Thesis

Field: Physics

Specialty: Medical Physics

Theme

Study of the relationship between radiation dose and image quality in computed tomography (CT)

Presented by : STOUTAH Youssera

Defended on:06/07/2026 before the jury composed of:

Sihem Djellab	MCA.	University of Skikda	President
Hayet Benzerouk	MCA	University of Skikda	Supervisor
Abdelhak Fekrache	MCB	University of Skikda	Examiner

Academic Year : 2025/2026

الشكر والتقدير

الحمدُ للهِ الذي بنعمته تتمُّ الصالحات، والذي أكرمني بفضله، وأعانني على إتمام هذا العمل، فله الحمدُ والشكرُ أولًا وآخرًا، ظاهرًا وباطنًا، حمدًا كثيرًا طيبًا مباركًا فيه، يليق بجلال وجهه وعظيم سلطانه.

ثم أتقدم بخالص الشكر والعرفان إلى والديَّ العزيزين، اللذين كانا بعد فضل الله تعالى النور الذي أضاء دربي، والسند الذي استندت إليه في كل مرحلة من مراحل حياتي. فما قدماه لي من حبٍّ وحنانٍ ورعايةٍ ودعاءٍ وتشجيعٍ وتضحياتٍ لا يمكن للكلمات أن توفيه حقه. أسأل الله أن يجزيهما عني خير الجزاء، وأن يحفظهما، ويبارك في عمرهما، ويديمهما نعمةً لا تزول.

كما أتوجه بخالص الشكر والعرفان إلى أختي العزيزة، وإلى أخويَّ العزيزين، على ما أحاطوني به من محبةٍ وتشجيعٍ ومساندةٍ صادقة، فكانوا خيرَ سندٍ وعونٍ لي طوال هذه المسيرة. أسأل الله أن يحفظهم، ويبارك فيهم، ويجزيهم عني خير الجزاء. والى كل من ساندني من عائلتي شكرا جزيلا.

كما أتقدم بالشكر إلى الأستاذة المشرفة الدكتورة **بن زروق حياة**، على إشرافها الأكاديمي ومتابعتها لهذا العمل.

وأتقدم بجزيل الشكر إلى الأستاذة رئيسة لجنة المناقشة الدكتورة **جلاب سهام**، وإلى الأستاذ المناقش الدكتور **فكراش عبد الحق**، على تفضلهما بقبول مناقشة هذه المذكرة، وما سيبذلانه من وقتٍ وجهدٍ في تقييمها، راجيًا أن ينال عملي استحسانهما.

لا يسعني إلا أن أعبر عن شكري وامتناني الكبيرين إلى الأستاذ الدكتور **مولود بوقجان**، الذي كان سندًا حقيقيًا لي، وناصحًا أمينًا، وداعمًا منذ أن بدأتُ دراسةَ تخصص الفيزياء الطبية. لقد كان لتوجيهاته السديدة، وتشجيعه المستمر، ووقوفه إلى جانبي بالغُ الأثر في مواصلة مسيرتي وإتمام هذا العمل، فله مني أسمى عبارات الشكر والتقدير، وأسأل الله أن يجزيه عني خير الجزاء.

كما أتقدم بخالص الشكر والتقدير مرة أخرى إلى الأستاذة الدكتورة الكريمة **جلاب سهام**، التي رافقتني منذ بداية مسيرتي الجامعية، وكانت مثالًا في التواضع وحسن الخلق. أشكر لها ما قدمته لي من دعم وتشجيع، ومواقفها الطيبة التي ستظل محل تقدير وامتنان، وأسأل الله أن يجزيها عني خير الجزاء، ويبارك في علمها وعملها.

كما أتقدم بخالص الشكر والتقدير إلى أساتذة كلية العلوم، الذين كانوا أكثر من مجرد أساتذة؛ فقد كانوا مصدرًا للدعم والتوجيه، فجزاهم الله عني خير الجزاء. عرفانًا بما قدموه لي من نصحٍ وتوجيهٍ وتشجيع، وبما تركوه من أثرٍ طيب في مسيرتي العلمية والإنسانية.

كما أتوجه بجزيل الشكر إلى جميع أساتذة تخصص الفيزياء الذين درسوني، فلهم الفضل، بعد الله تعالى، في تكويني العلمي، وأسأل الله أن يبارك في علمهم ويجزيهم عني خير الجزاء.

وأشكر كل أستاذ درسني، وترك في نفسي أثرًا طيبًا، ولو بكلمة صادقة أو نصيحة مخلصة.

كما أتقدم بخالص الشكر والامتنان إلى جميع أفراد طاقم مصلحة التصوير المقطعي المحوسب(CT) ، وإلى كل من ساندني وساعدني من العاملين بمركز مكافحة السرطان، بالمؤسسة الاستشفائية الجامعية ابن رشد عنابة، تقديرًا لحسن استقبالهم، وتعاونهم المثمر والطيب، وما أبدوه من دعم وتسهيلات طوال فترة التربص، مما أسهم في تهيئة بيئة علمية مناسبة كان لها بالغ الأثر في إنجاز هذا العمل.

ولا يفوتني أن أشكر نفسي؛ تلك النفس الطموحة، الصبورة، المثابرة، التي لم تستسلم يومًا أمام الصعوبات، وظلت تؤمن بأن لكل تعبٍ ثمرة، ولكل اجتهادٍ نجاحًا. شكرًا لها لأنها واصلت الطريق رغم التحديات، وتحملت المشاق، وثابرت بإيمان وعزيمة حتى بلغت هذه اللحظة. والحمد لله على توفيقه وفضله، فما كان لهذا الإنجاز أن يكتمل لولا عونه سبحانه.

وإلى كل من كان له أثرٌ طيب في مسيرتي، ولم تسعفني الكلمات لذكره، أقول: جزيل الشكر والامتنان، وجزاكم الله عني خير الجزاء.

الإهداء

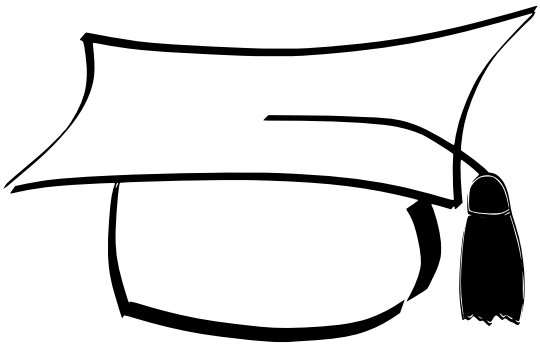
إلى أغلى ما أملك في هذه الحياة، إلى من كانا نبع الحب الذي لا ينضب، إلى من كانا سندي، الى من افخر بكونهم والدي، إلى من أحسنا تربيتي، وربّياني على الخير، ونهَياني عن الشر والفتنة والنفاق...

- **إلى أبي الغالي**، رمز القوة والعطاء، الذي كان لي قدوةً في الصبر والعطاء، إلى من علمني أن بعد الضيق فرج، وأن لكل شدةٍ مدة.
- **وإلى أمي الحبيبة**، التي كان دعاؤها سرَّ توفيقي ونجاحي، وحنانها ملاذي في كل محطة، وشاركتني عناء هذه الرحلة يومًا بيوم.
- **وإلى أختي الغالية، وإلى أخويَّ العزيزين**، رفقاء الدرب، ومصدر الفرح والسند، الذين كانوا دائمًا إلى جانبي في السراء والضراء.
- **وإلى نفسي ...**تلك التي آمنت بالحلم رغم الصعاب، وواصلت السير رغم التعب، ولم تتوقف عن الاجتهاد حتى بلغت هذه اللحظة.

أهدي إليكم جميعًا ثمرة هذا الجهد، وحصاد سنواتٍ من الدراسة والاجتهاد، سائلةً الله أن يجعل هذا العمل سببًا لرضاه، وأن يديم عليكم الصحة والسعادة، ويبارك في أعماركم.

﴿وَآخِرُ دَعْوَاهُمْ أَنِ الْحَمْدُ لِلَّهِ رَبِّ الْعَالَمِينَ﴾

سورة يونس: 10



ملخص

مع التوسع المستمر في استخدام التصوير المقطعي المحوسب **(Computed Tomography, CT)**، أصبح تحقيق التوازن بين تقليل الجرعة الإشعاعية والمحافظة على جودة الصورة التشخيصية أحد أهم التحديات في الفيزياء الطبية والتصوير التشخيصي. ويستند هذا النهج إلى مبدأ **ALARA (As Low As Reasonably Achievable)**، الذي يوصي باستخدام أقل جرعة إشعاعية ممكنة مع الحفاظ على جودة صورة تشخيصية كافية تضمن دقة التشخيص وسلامة المرضى، مما يسهم في الحد من المخاطر البيولوجية الناتجة عن التعرض غير الضروري للإشعاع المؤين.

تهدف هذه الدراسة إلى تحليل العلاقة بين الجرعة الإشعاعية وجودة الصورة في فحوصات التصوير المقطعي المحوسب للصدر والبطن والحوض **(Thoraco-Abdomino-Pelvic Computed Tomography, TAP CT)** خلال المرحلة الوريدية البابية، مع تقييم تأثير بعض العوامل الديموغرافية والتقنية، مثل العمر والجنس وقيمة **mAs**، على الجرعة الإشعاعية ومؤشرات جودة الصورة.

أُجريت هذه الدراسة بالمصلحة المركزية للأشعة في **المستشفى الجامعي ابن رشد بعنابة**، تحت إشراف الطاقم التقني للمصلحة، باستخدام جهاز **SCENARIA View Whole Body X-ray CT System** المصنع من طرف **FUJIFILM Corporation (Japan).** وشملت الدراسة **12 مريضًا** خضعوا لفحص **TAP CT**، منهم **6 رجال و6 نساء**. واعتمد التحليل على دراسة مؤشرات الجرعة الإشعاعية المتمثلة في **CTDIvol** و**DLP**، بالإضافة إلى تقييم جودة الصورة موضوعيًا باستخدام مؤشرات **Noise** و**Signal-to-Noise Ratio (SNR)** و**Contrast-to-Noise Ratio (CNR)**. وقد تراوحت قيم **CTDIvol** بين **6.4** و **8.9mGy**، بينما تراوحت قيم **DLP** بين **486.4** و**677.7mGy·cm**.

أظهرت نتائج تحليل الانحدار الخطي أن العلاقة بين العمر والجرعة الإشعاعية كانت ضعيفة، حيث بلغت معاملات التحديد **(R^2) 0.1403** لدى الذكور و **0.1468** لدى الإناث، مما يشير إلى أن العمر يفسر جزءًا محدودًا من التباين في الجرعة الإشعاعية داخل عينة الدراسة، مع ضرورة الاستناد إلى اختبارات الدلالة الإحصائية للحكم النهائي على معنوية هذه العلاقة. وفي المقابل، أظهرت النتائج علاقة خطية قوية بين قيمة **mAs** ومؤشر **CTDIvol**، حيث بلغت قيمة **R^2 = 0.9135** لدى الذكور و **R^2 = 0.9879** لدى الإناث، وهو ما يتوافق مع المبادئ الفيزيائية للتصوير المقطعي، إذ تؤدي زيادة قيمة **mAs** إلى زيادة عدد فوتونات الأشعة السينية المنبعثة، وبالتالي ارتفاع الجرعة الإشعاعية الممتصة.

كما أظهرت الدراسة اختلاف قوة العلاقة بين الجرعة الإشعاعية ومؤشرات جودة الصورة. فقد بلغت قيمة **R^2** لمؤشر Noise **0.8769** لدى الذكور و**0.2639** لدى الإناث، بينما بلغت **0.5911** لدى الذكور و**0.5752** لدى الإناث بالنسبة لمؤشر **SNR**، و **0.6222** لدى الذكور و **0.3710** لدى الإناث بالنسبة لمؤشر **CNR**. وتشير هذه النتائج إلى أن تأثير الجرعة الإشعاعية على جودة الصورة يختلف باختلاف المؤشر المدروس، كما قد يتأثر بعوامل تقنية مرتبطة ببروتوكول التصوير، إضافة إلى خصائص المرضى وتباين أحجام أجسامهم، الأمر الذي يستدعي تفسير هذه النتائج في ضوء المعطيات الفيزيائية والإكلينيكية.

وتؤكد هذه الدراسة أن جودة الصورة في التصوير المقطعي المحوسب لا تعتمد على الجرعة الإشعاعية وحدها، بل تتأثر أيضًا بمجموعة من العوامل التقنية، مثل سمك الشرائح، وخوارزميات إعادة بناء الصورة، وتقنيات تقليل الضوضاء، فضلًا عن العوامل المرتبطة بالمريض، مثل حجم الجسم ومؤشر كتلة الجسم عند توفر هذه البيانات. وتبرز النتائج أهمية تحسين بروتوكولات التصوير واختيار المعلمات التقنية المثلى لتحقيق أفضل توازن بين جودة الصورة التشخيصية وتقليل

الجرعة الإشعاعية، بما يتوافق مع مبادئ الحماية الإشعاعية ومبدأ **ALARA**، مع الإشارة إلى أن صغر حجم العينة في هذه الدراسة يستدعي إجراء دراسات مستقبلية تشمل عددًا أكبر من المرضى لتعزيز القوة الإحصائية وإمكانية تعميم النتائج.

الكلمات المفتاحية :التصوير المقطعي المحوسب(CT) ، الجرعة الإشعاعية، جودة الصورة، TAP CT، CTDIvol، DLP، Noise، SNR، CNR، ALARA.

Abstract

The increasing use of computed tomography (CT) has raised growing concerns about balancing radiation dose reduction with the preservation of diagnostic image quality. This challenge is addressed through the **As Low As Reasonably Achievable (ALARA)** principle, which advocates minimizing radiation exposure while maintaining sufficient image quality for accurate diagnosis and patient safety.

This study aimed to investigate the relationship between radiation dose and image quality in thoraco-abdomino-pelvic computed tomography (**TAP CT**) examinations performed during the portal venous phase. In addition, the effects of demographic and technical factors, including age, sex, and tube current-time product (**mAs**), on radiation dose and image quality were evaluated.

The study was conducted at the Central Radiology Department of **Ibn Rochd University Hospital**, Annaba, Algeria, using a **SCENARIA View Whole Body X-ray CT System** (FUJIFILM Corporation, Japan). A total of **12 patients** (6 males and 6 females) who underwent TAP CT examinations were included. Radiation dose was assessed using the **Computed Tomography Dose Index volume (CTDIvol)** and **Dose-Length Product (DLP)**, while objective image quality was evaluated using **Noise**, **Signal-to-Noise Ratio (SNR)**, and **Contrast-to-Noise Ratio (CNR)**. CTDIvol values ranged from **6.4 to 8.9 mGy**, whereas DLP values ranged from **486.4 to 677.7 mGy·cm**.

Linear regression analysis showed a weak association between age and radiation dose, with coefficients of determination (R^2) of **0.1403** for males and **0.1468** for females, indicating that age explained only a small proportion of the variability in radiation dose within the study population. In contrast, a strong positive correlation was observed between **mAs** and **CTDIvol**, with $R^2 = 0.9135$ for males and $R^2 = 0.9879$ for females, confirming the expected increase in radiation dose with increasing tube current-time product.

The relationship between radiation dose and image quality varied according to the evaluated metric. For **Noise**, the coefficients of determination were **0.8769** in males and **0.2639** in females. For **SNR**, the corresponding values were **0.5911** and **0.5752**, while **CNR** showed R^2 values of **0.6222** and **0.3710** for males and females, respectively. These findings suggest that image quality is influenced not only by radiation dose but also by technical acquisition parameters and patient-related characteristics.

Overall, the results demonstrate that optimizing CT protocols requires consideration of multiple factors beyond radiation dose alone. Appropriate selection of acquisition parameters can improve diagnostic image quality while minimizing radiation exposure in accordance with

the **ALARA** principle. Nevertheless, the relatively small sample size warrants further studies involving larger patient populations to strengthen the statistical power and improve the generalizability of the findings.

Keywords: Computed Tomography (CT); Radiation Dose; Image Quality; ALARA; Thoraco-Abdomino-Pelvic CT (TAP CT); CTDIvol; Dose-Length Product (DLP); Signal-to-Noise Ratio (SNR); Contrast-to-Noise Ratio (CNR).

Table of Contents

List of Tables IV
List of Figures V
List of Abbreviations VII
List of Symbols VIII
General Introduction 1

Chapter 01

Bibliographic Study

1 Introduction 4
2 Radiation 4
2.1 Classification of Radiation 4
2.1.1 Non-ionizing radiation 4
2.1.2 Ionizing radiation 4
2.2 Type of radiation 5
2.2.1 Particulate Radiation 5
2.2.2 Electromagnetic Radiation 5
2.3 Sources of Radiation 9
2.3.1 Natural Sources of Radiation 9
2.3.2 Artificial Sources of Radiation 9
2.4 Spectrum and Classification of Electromagnetic Radiation 10
3 Interaction of X-Rays with Matter 11
3.1 Photon Beam Attenuation 11
3.2 Coherent (Rayleigh) Scattering 12
3.3 Photoelectric Effect 12
3.4 Pair production 13
4 Dosimetry 14
4.1 Absorbed Dose 15
4.2 Equivalent Dose 15
4.3 Effective Dose 16
4.4 Importance of dosemetry 17
5 Medical Imaging Systems Using X-rays 17
5.1 Diagnostic Applications 17
5.1.1 Conventional Radiography 17
5.1.2 Fluoroscopy 18
5.1.3 Mammography 18
5.1.4 Angiography 19
5.1.5 Computed Tomography (CT) 19

5.2 Therapeutic Applications 20
5.2.1 Radiotherapy 20
6 Radiation Protection 21
6.1 Basic Principles of Radiation Protection 21
6.1.1 Justification 21
6.1.2 Optimization (ALARA) 21
6.1.3 Dose limits 21
6.2 Diagnostic Reference Levels (DRLs) 22
7 Conclusion 22

Chapter II

Materials and Methods

1 Introduction 24
2 Presentation of the Medical Imaging Department 24
3 CT Scanner Used in the Study 25
4 CT Principle 25
5 CT Scanner Components 26
5.1 Generator 26
5.2 Gantry 26
5.3 X-ray Tube 26
5.4 Detectors 27
5.5 Radiation Shielding Elements 27
5.6 Patient Table 27
5.7 Image Processor 27
5.8 Control Console 27
6.1 Study Type 28
6.2 Study Sample and Characteristics 28
6.3 Study Conditions 29
7 Triphasic CT Protocol for Thoraco-Abdomino-Pelvic Imaging 30
7.1 Patient Preparation for a Triphasic TAP CT Examination 30
7.2 Before the Examination 30
7.3 Special Precautions in Certain Cases 31
7.4 Patient Positioning During the Examination 31
7.5 Special Cases 32
7.6 After the Examination 33
8 Contrast Media 33
9 Imaging Phases of a Multiphase TAP CT Examination 34
9.1 Phases of a Triphasic TAP CT Examination 34

9.1.1 Non-Contrast Phase 34
9.1.2 Arterial Phase 34
9.1.3 Portal Venous Phase 35
9.1.4 Delayed Phase 35
9.2 Contrast Injection Considerations 36
10 Radiation Dose Indicators 36
10.1 Computed Tomography Dose Index Volume (CTDIvol) 37
10.2 Dose-Length Product (DLP) 37
10.3 Effective Dose (E) 37
11 Image Quality Assessment 37
11.1 Fundamental Concepts of Image Quality in CT 38
11.1.1 Spatial resolution 39
11.1.2 Contrast resolution 39
11.1.3 Noise 40
11.1.4 Image artifacts 40
11.2 Quantitative Image Quality Metrics in CT 40
11.2.1 Signal-to-noise ratio (SNR) 40
11.2.2 Contrast-to-noise ratio (CNR) 41
11.2.3 Advanced Image Quality Metrics 41
11.3 Influence of CT Technical Parameters and Patient Factors on Image Quality and Radiation Dose 42
11.3.1 Tube Current- Time Product (mAs) 42
11.3.2 Patient Positioning 42
11.3.3 Pitch 43
11.3.4 Slice Thickness (dose-focused) 43
11.3.5 Scan Range (Scan Length) 43
11.3.6 Tube Voltage (kVp) 43
11.3.7 Patient size (BMI, weight, and height) 44
11.3.8 Age 44
12 Dose Reduction and Radiation Protection in Computed Tomography (CT) 44
12.1 Modern Equipment Technologies 44
12.1.1 Automatic Exposure Control (AEC) 44
12.1.2 Organ-Based Tube Current Modulation (OTCM) 44
12.1.3 Image Quality Improvement at Low Doses 45
12.2 Radiation Protection Procedures 45
12.2.1 Use of Protective Devices for Sensitive Organs 45
12.2.2 Limitation of Scan Range 45

12.2.3 Selection of the Appropriate Scanning Protocol 45
12.2.4 Justification of Examination 45
12.2.5 Optimization 46
13 Impact of Image Quality on Diagnosis 46
14 Conclusion 46

Chapter III

Results and Discussion

1 Introduction 49
2 Radiation Dose Analysis 49
2.1 Effect of Age on Radiation Dose Accoeding to sex 50
2.1.1 CTDIvol 50
2.1.2 DLP 52
2.2 Effect of mAs on Radiation Dose 54
3 Comparison of Radiation Dose According to Examination Type : 55
4 Image Quality Analysis 57
4.1 Noise Analysis 57
4.2 SNR Analysis 58
4.3 CNR Analysis 58
5 Relationship Between Radiation Dose and Image Quality 59
5.1 Relationship Between Dose and Noise 60
5.2 Relationship Between Dose and SNR 61
5.3 Relationship Between Dose and CNR: 62
5.3.1 Comparison with Previous Studies 63
6 Conclusion 64
General Conclusion 65
References 68

List of Tables

Table I.1: Comparison between ionizing and non-ionizing radiation…….……5

Table I. 2: Tissue weighting factors (WR) for different types of radiation 16

Table I. 3: Publication 103 (ICRP, 2007a) tissue weighting factors 166

Table II.1: Demographic Characteristics of the Patients 289

Table III.1 : Patient demographic characteristics and radiation dose parameters for TAP CT examinations in the portal venous phase..... 50

Table III.2 : Comparison of CTDIvol and DLP Values Between TAP CT (Portal Venous Phase) and Brain APC CT Examinations..... 56

Table III.3 : Patient image noise measurements during CT examinations 57

Table III.4 : Patient SNR measurements during CT examinations 58

Table III.5 : Patient CNR measurements during CT examinations 59

Table III.6 : CTDIvol and image quality metrics (Noise, SNR, CNR) in CT examinations.. 60

List of Figures

Figure I.1 : Classification of Radiation 6
Figure I.2 : One of the first X-rays, taken from Wilhelm Röntgen of his wifes hand 7
Figure I.3 : Structure of an X-ray Tube 8
Figure I.4 : Mechanisms of X-ray Production 9
Figure I.5 : The principal natural and artificial sources of radiation……10
Figure I.6 : The electromagnetic spectrum 11
Figure I.7 : Inelastic (Compton) scatter 122
Figure I.8 : The photoelectric interaction 133
Figure I.9 : Pair Production 144
Figure I.10 : Photon interection with matter diagram 144
Figure I.11: Chest examination using conventional radiography 177
Figure I.12: Fluoroscopy machine……...18
Figure I.13: Mammography Machine 18
Figure I.14: Angiography Machine……19
Figure I.15 : Computed Tomography (CT) Scanner 20
Figure I.16: Radiotherapy Uni 21
Figure II.1 : CT scanner used for this study at Ibn Rochd University Hospital, Annaba 255
Figure II.2 : Some components of the CT scanner used in this study 288
Figure II. 3 : CT scout (topogram) image for scan range planning 332
Figure II.4 : Patient positioning during a TAP CT examination 332
Figure II.5 : Contrast media used during the CT examination 33
Figure II.6 : Liver CT image in the non-contrast phase 34
Figure II.7 : Liver CT image in the arterial phase 35
Figure II.8 : Liver CT image in the portal venous phase 35
Figure II.9 : CT dose report of the examination 366
Figure II.10 : Methodology for region of interest (ROI) placement and liver image analysis in the portal venous phase 388
Figure III.1 : Relationship between Age and CTDIvol According to Sex in Portal Venous Phase TAP CT Examinations 51
Figure III.2 : Relationship between Age and DLP According to Sex in Portal Venous Phase TAP CT Examinations 53
Figure III.3 : Scout images of patients 8, 12, and 7, respectively. 53

Figure III.4: Scout images of patients 1, 3, and 5, respectively. 53
Figure III. 5 : Relationship Between mAs and CTDIvol According to Sex..... 55
Figure III.6: Scout images of contrast-enhanced brain CT and TAP CT in the portal venous phase..... 57
Figure III.7 : Relationship between CTDIvol and Noise during TAP CT examinations (portal venous phase) 61
Figure III.8 : Relationship between CTDIvol and SNR during TAP CT examinations (portal venous phase) 62
Figure III.9 : Relationship between CTDIvol and CNR during TAP CT examinations (portal venous phase) 63

List of Abbreviations

Abbreviation	Meaning
AEC	Automatic Exposure Control
ALARA	As Low As Reasonably Achievable
APC	Arterial–Portal–Contrast phase CT (avec produit de contraste)
ATCM	Automatic Tube Current Modulation
CNR	Contrast-to-Noise Ratio
CT	Computed Tomography
CTDIvol	Volume Computed Tomography Dose Index
DLP	Dose-Length Product
DRL	Diagnostic Reference Level
FBP	Filtered Back Projection
HU	Hounsfield Unit
IAEA	International Atomic Energy Agency
ICRP	International Commission of Radiological Protection
MBIR	Model-Based Iterative Reconstruction
MDCT	Multi-Detector Computed Tomography
MRI	Magnetic Resonance Imaging
MTF	Modulation Transfer Function
NPS	Noise Power Spectrum
ROI	Region of Interest
SNR	Signal-to-Noise Ratio
TAP	Thoraco-Abdomino-Pelvic CT

List of Symbols

Symbol	Meaning	Unit
CNR	Contrast-to-Noise Ratio	—
CTDIvol	CT dose index	mGy
D	Absorbed dose	Gy
DLP	Dose-Length Product	mGy·cm
E	Effective dose	Sv
H	Planck constant	J·s
HT	Equivalent dose	Sv
HVL	Half-Value Layer	mm
I_0	Incident intensity	—
I(x)	Transmitted intensity	—
K	Conversion coefficient	mSv/(mGy·cm)
kVp	Peak tube voltage	kV
Λ	Wavelength	m
M	Linear attenuation coefficient	cm^{-1}
$\bar{\mu}$	Mean signal intensity	HU
mAs	Tube current–time product	mA·s
N	Frequency	Hz
R^2	Coefficient of determination	—
S_1, S_2	ROI signal intensities	HU
SNR	Signal-to-Noise Ratio	—
Σ	Image noise (standard deviation)	HU
TVL	Tenth-Value Layer	mm
X	Material thickness	mm / cm
Z	Atomic number	—

General Introduction

Computed Tomography (CT) has become one of the most important diagnostic imaging modalities in modern medicine. It provides rapid acquisition of high-resolution cross-sectional images, allowing accurate visualization of internal anatomical structures and facilitating the diagnosis of a wide range of diseases. Owing to its speed, accessibility, and high diagnostic performance, CT is routinely used for abdominal, thoracic, and pelvic (TAP) examinations in clinical practice.

Despite its undeniable clinical benefits, the growing use of CT has substantially increased patient exposure to ionizing radiation, making radiation protection a major concern in medical imaging. To minimize potential radiation risks while preserving diagnostic performance, the **ALARA (As Low As Reasonably Achievable)** principle recommends using the lowest radiation dose that can produce images of sufficient diagnostic quality. Consequently, optimizing CT protocols requires achieving an appropriate balance between radiation dose and image quality, as increasing radiation exposure generally reduces image noise and improves image quality, whereas excessive dose reduction may compromise diagnostic accuracy.

Over the past decades, numerous studies have investigated radiation dose reduction techniques and image quality assessment in CT. However, relatively limited evidence is available regarding their combined evaluation in routine clinical practice during abdominal, thoracic, and pelvic examinations performed in the portal venous phase. In particular, further investigation is needed to better understand how radiation dose indicators, such as CTDIvol and DLP, relate to objective image quality parameters while considering both technical acquisition settings and patient characteristics. Improving this understanding may contribute to the development of more effective dose optimization strategies without compromising diagnostic confidence.

The present study aims to investigate the relationship between radiation dose and image quality in TAP CT examinations acquired during the portal venous phase. More specifically, it evaluates radiation dose indicators (CTDIvol and DLP) in relation to objective image quality metrics, including image noise, signal-to-noise ratio (SNR), and contrast-to-noise ratio (CNR). In addition, the study examines the influence of selected demographic and technical factors on these parameters.

This study was conducted using clinical CT examinations collected from patients at the Medical Imaging Department of Ibn Rochd Hospital, Annaba, during a clinical internship.

Radiation dose and image quality parameters were measured and statistically analyzed to investigate the relationship between radiation exposure and diagnostic image quality.

This master's thesis is organized into three chapters. **The first chapter** presents the theoretical background of ionizing radiation, X-ray production, CT imaging principles, radiation dose concepts, image quality, radiation protection, and the ALARA principle. **The second chapter** describes the study design, materials, and methodology used for data collection and quantitative analysis. **The third chapter** presents the obtained results, discusses the relationship between radiation dose and image quality, evaluates the influence of demographic and technical factors, and compares the findings with previously published studies.

Overall, this study contributes to a better understanding of the relationship between radiation dose and image quality in CT imaging. The findings are expected to provide practical evidence that may support dose optimization strategies, thereby improving patient radiation protection while maintaining the diagnostic quality required for routine clinical practice.

Chapter 01

Bibliographic Study

1 Introduction

Radiation is a physical phenomenon that has been studied since the late nineteenth century. The discovery of X-rays in 1895 by Wilhelm Conrad Röntgen **[1]** marked a major step in medicine, as it made it possible to see inside the human body without surgery, improving both diagnosis and treatment.

Today, X-rays are widely used in medical imaging, particularly in conventional radiography, mammography, and computed tomography (CT). These techniques produce detailed images of internal organs and tissues, supporting more accurate diagnosis.

Since ionizing radiation can affect the human body, careful dose management and a solid understanding of its physical properties are necessary. For this reason, a balance must always be maintained between the medical benefits and potential risks.

This chapter presents the main concepts of this study, including radiation types and sources, X-ray production, interactions with matter, dosimetry, medical applications, and radiation protection.

2 Radiation

Radiation is energy emitted from unstable atoms or produced by devices, which then travels through space or through a material medium in the form of electromagnetic waves or energy-carrying particles **[2]**.

2.1 Classification of Radiation

Radiation can be classified into ionizing and non-ionizing types, depending on how it interacts with matter **[3; 4]**.

2.1.1 Non-ionizing radiation

Non-ionizing radiation does not possess enough energy to ionize matter, since its energy per quantum is lower than the ionization energy of atoms (such as radio waves and microwaves) **[3; 4]**.

2.1.2 Ionizing radiation

Ionizing radiation is radiation with sufficient energy to remove electrons from atoms or molecules, thereby producing ions. This occurs because the energy carried by each quantum exceeds the ionization energy of the atoms in the irradiated material.

Ionizing radiation is classified into two main categories: **directly ionizing radiation** and **indirectly ionizing radiation**.

Directly ionizing radiation consists of charged particles, such as alpha particles, beta particles (electrons), protons, and heavy ions, which transfer their energy directly to matter through Coulomb interactions with atomic electrons.

In contrast, indirectly ionizing radiation consists of uncharged particles, such as X-rays and gamma rays, which first interact with matter to produce secondary charged particles that subsequently ionize atoms through Coulomb interactions. Owing to their ability to penetrate biological tissues and deposit energy within them, ionizing radiations are widely used in medical diagnosis and radiation therapy, although their use requires careful radiation protection because of their potential biological effects **[3,4].**

The following table presents a comparison between ionizing and non-ionizing radiation

Table I.1 Comparison between ionizing and non-ionizing radiation

Aspect	Ionizing Radiation	Non-Ionizing Radiation
Energy	High	Low
Effect on atoms	Ionizes atoms by removing electrons	Excites atoms without ionization
Biological effects	May damage DNA and cells	Mainly causes heating; no direct DNA ionization
Examples	X-rays, Gamma rays, Radon	Visible light, Infrared, Radio waves, Microwaves
Medical applications	Radiography, CT, Nuclear Medicine, Radiotherapy	MRI, Laser therapy

2.2 Type of radiation

2.2.1 Particulate Radiation

Particulate radiation is radiation in the form of massive particles. Examples include alpha particles and beta particles **[2]**.

2.2.2 Electromagnetic Radiation

Electromagnetic radiation travels as waves, including radio waves, visible light, and X-rays. Its energy is inversely related to wavelength and is carried by photons. High-energy radiation such as X-rays and gamma rays is ionizing because it can remove electrons from atoms**[4]**. Figure I.1 presents a general classification of radiation.

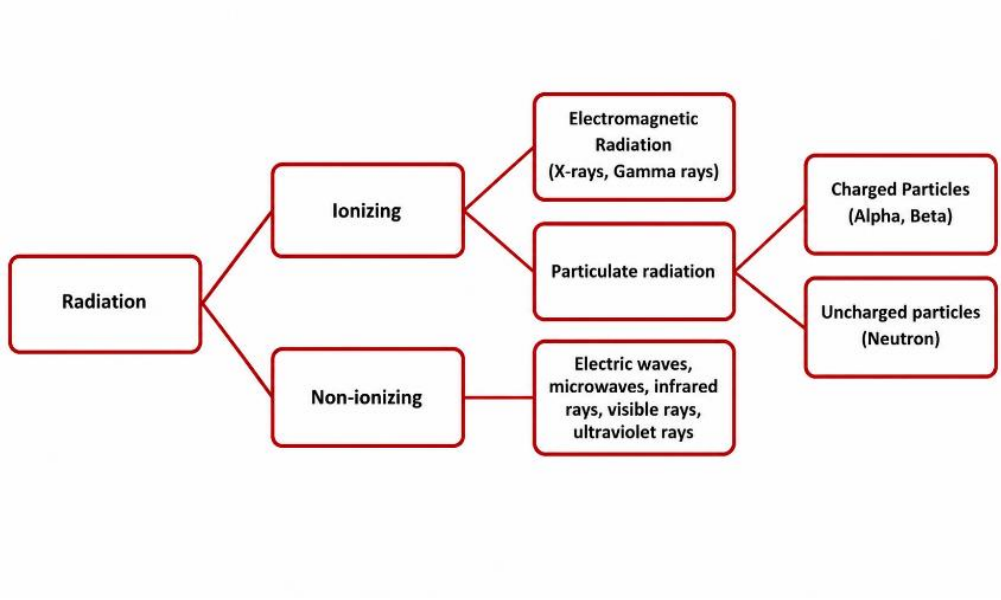


Figure I.1 : Classification of Radiation

2.2.2.1 X-rays

2.2.2.1.1 History of X-rays

The history of X-rays began in **1895** when the German scientist **Wilhelm Conrad Röntgen** was conducting experiments on a cathode ray tube in his laboratory at the University of Würzburg. During his work, he noticed an invisible radiation capable of penetrating certain materials and causing a nearby screen to glow, which led him to realize that he had made a new discovery. Since the nature of this radiation was unknown, he named it **X-rays [1]**. A few weeks after this discovery, Röntgen produced the first medical X-ray image of his wife Bertha's hand, clearly showing the bones and her ring. This image marked the birth of radiography and became a major turning point in medical history **[1]**. Figure I.2 presents one of the earliest X-ray images, captured by Wilhelm Röntgen of his wife's hand.



Figure I.2 : One of the first X-rays, taken from Wilhelm Röntgen of his wife hand **[5]**

News of the discovery spread rapidly, and doctors in many countries began using X-rays to detect fractures, injuries, and foreign objects inside the body. This greatly improved the speed and accuracy of medical diagnosis. X-rays remain one of the most important tools in medicine worldwide**[6].**

In **1901**, Röntgen received the first Nobel Prize in Physics in recognition of his remarkable discovery. Over the years, X-ray machines became safer and more precise, followed by modern technologies such as digital radiography and computed tomography. Today, X-rays are among the most essential tools in modern medical diagnosis**[1]**.

2.2.2.1.2 Definition of X-rays

X-rays are defined as a type of ionizing electromagnetic radiation that travels in the form of waves or high-energy photons. They are characterized by their ability to penetrate materials to different degrees. For this reason, they are widely used in the medical field, especially for diagnosis and radiographic imaging, as well as in some industrial and scientific applications **[7]**.

The main characteristics of this radiation are as follows:

1. Frequency (ν): ranges between 10^{16} Hz and 10^{20} Hz.
2. Wavelength (λ): ranges approximately from 0.1 nm to 10 nm.

3. Energy (E): it is a quantized and well-defined energy, measured in joules (J), but it is more commonly expressed in electron volts (eV).

4. Energy relation: the energy is related to frequency and wavelength by the following equation:

$$E = \frac{h \times C}{\lambda} = h\vartheta \qquad \text{I. 1}$$

Where:

h is Planck's constant, equal to 6.626×10^{-34} J·s.

c is the speed of light in vacuum, equal to 3×10^{8} m/s **[8]**.

2.2.2.1.3 Production of X-rays

X-rays are produced in an X-ray tube that contains a cathode and an anode inside a vacuum. Electrons are emitted from the heated cathode through thermionic emission and are accelerated toward the anode by a high voltage.

When the electrons strike the anode, most of their energy is converted into heat, while a small part is transformed into X-rays. The amount and energy of the produced X-rays depend mainly on the tube current and the applied voltage. Figure I.3 illustrates the structure of an X-ray tube.

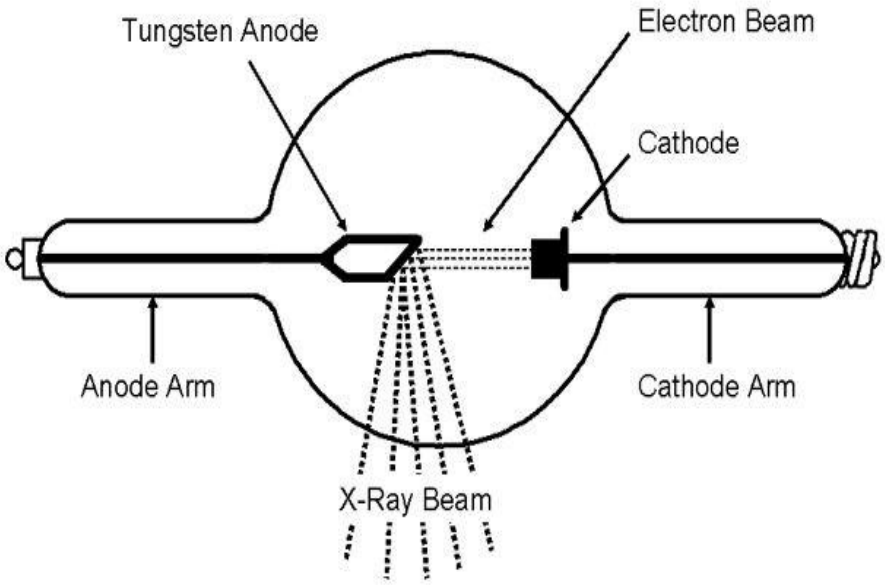


Figure I.3 : Structure of an X-ray Tube **[9]**

X-ray production occurs mainly through two mechanisms: Bremsstrahlung radiation, which is produced when electrons are decelerated near atomic nuclei, and characteristic radiation, which occurs when inner-shell electron vacancies are filled by outer-shell electrons, releasing photons with specific energies.

Since most of the energy is converted into heat, cooling systems and beam filtration are used to improve tube performance and control the quality of the X-ray beam**[10]**. Figure I.4 illustrates Mechanisms of X-ray Production.

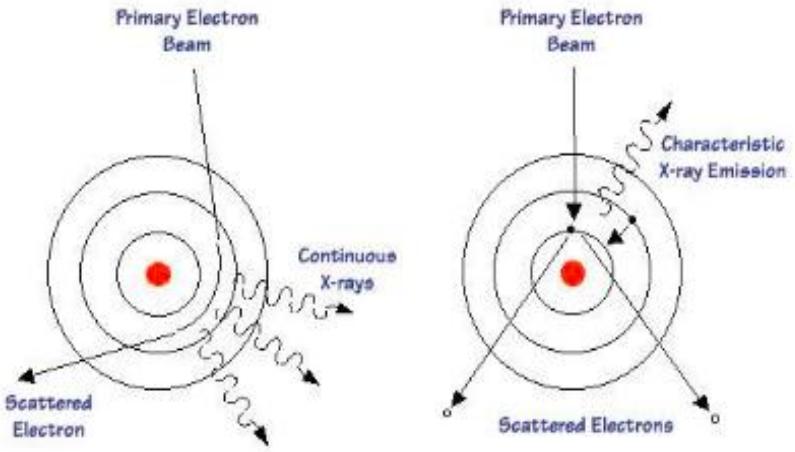


Figure I.4 : Mechanisms of X-ray Production **[11]**

2.3 Sources of Radiation

Radiation is present everywhere in the environment. Most of it comes from natural sources, while a smaller part is produced by human activities. Natural radiation is known as background radiation **[8]**.

2.3.1 Natural Sources of Radiation

Background radiation is a natural type of radiation that is always present in the environment. It is the main source of human exposure to radiation. It is classified into three types. Cosmic radiation comes from high-energy particles in space and becomes stronger at higher altitudes. Terrestrial radiation comes from radioactive elements found in soil and rocks, such as uranium-238, radium-226, radon, and potassium-40. Internal radiation comes from radioactive substances that enter the body through food or air, including potassium-40, carbon-14, and rubidium-87 **[8]**.

2.3.2 Artificial Sources of Radiation

Human exposure to radiation also comes from artificial sources, including medical use, industrial activities, and some consumer products. A small number of people work in environments where radiation sources are directly present.

In the past, nuclear weapons testing in the atmosphere was a major source of artificial radiation, but it has mostly stopped today, and its effect is now very limited **[8]**.

Some everyday products, such as smoke detectors and building materials, contain low levels of radiation. Air travel also increases exposure to cosmic radiation. The main source of artificial exposure is medical applications, especially diagnostic imaging, radiotherapy, and nuclear medicine, where radiation is used for diagnosis or treatment. Industrial sources include uranium mining, nuclear power plants, and the handling of radioactive materials. These activities may expose workers in medicine, aviation, and research to different levels of radiation **[8]**. The following figure presents the principal natural and artificial sources of radiation

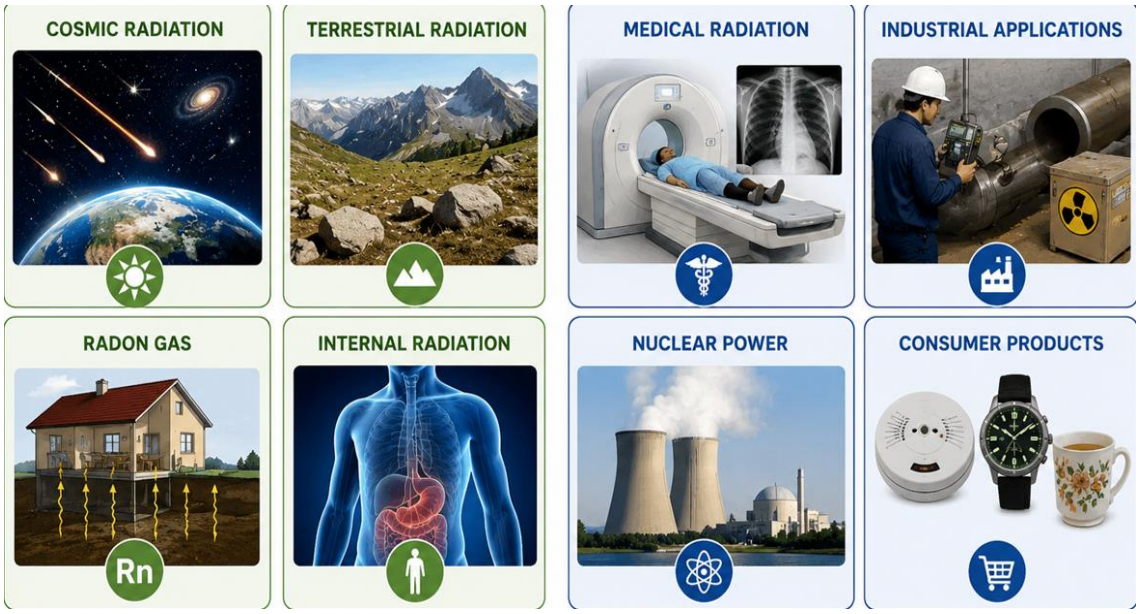


Figure I.5: the principal natural and artificial sources of radiation.

2.4 Spectrum and Classification of Electromagnetic Radiation

The electromagnetic spectrum represents the distribution of electromagnetic waves according to their wavelength, frequency, or energy. Figure I.6 presents an overview of the electromagnetic spectrum.

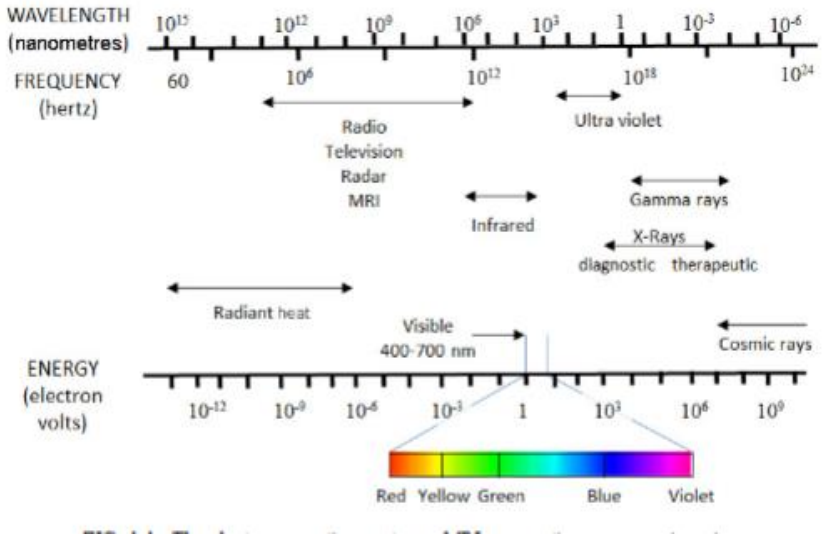


Figure I.6 : The electromagnetic spectrum[10]

3 Interaction of X-Rays with Matter

3.1 Photon Beam Attenuation

When X-rays pass through matter, their intensity decreases due to absorption and scattering. This attenuation follows the exponential law:

$$I(x) = I_0 e^{-\mu x} \qquad \text{I. 2}$$

where:

- I_0: the beam intensity before entering the material.
- $I(x)$: the beam intensity after passing through a thickness (x) of the material.
- μ: the linear attenuation coefficient, which depends on the photon energy $h\vartheta$ and the atomic number (Z) of the absorbing material.

The attenuation of X-rays is commonly described using:

Half-Value Layer (HVL): the thickness required to reduce the beam intensity to one-half. It is given by:

$$HVL = x_{\frac{1}{2}} = \frac{\ln(2)}{\mu} \qquad \text{I. 3}$$

- **Tenth-Value Layer (TVL):** the thickness required to reduce the beam intensity to one-tenth. It is expressed as

$$TVL = x_{\frac{1}{10}} = \frac{\ln(10)}{\mu} \qquad \text{I. 4}$$

[14].

3.2 Coherent (Rayleigh) Scattering

Coherent (Rayleigh) scattering occurs when an X-ray photon interacts with a bound electron and is scattered without significant energy loss. It is an elastic process and usually occurs at small angles.

This type of scattering contributes slightly to X-ray attenuation, but its effect in tissues is very small compared to the photoelectric effect and Compton scattering**[14]**.

Compton scattering occurs when an X-ray photon interacts with a loosely bound electron, transferring part of its energy to the electron. As a result, the photon is deflected with reduced energy, and the electron is emitted with kinetic energy.

This interaction is important in low atomic number materials and represents one of the main mechanisms of X-ray interaction with matter in diagnostic energy ranges **[14] ,**As shown in Figure I.7 .

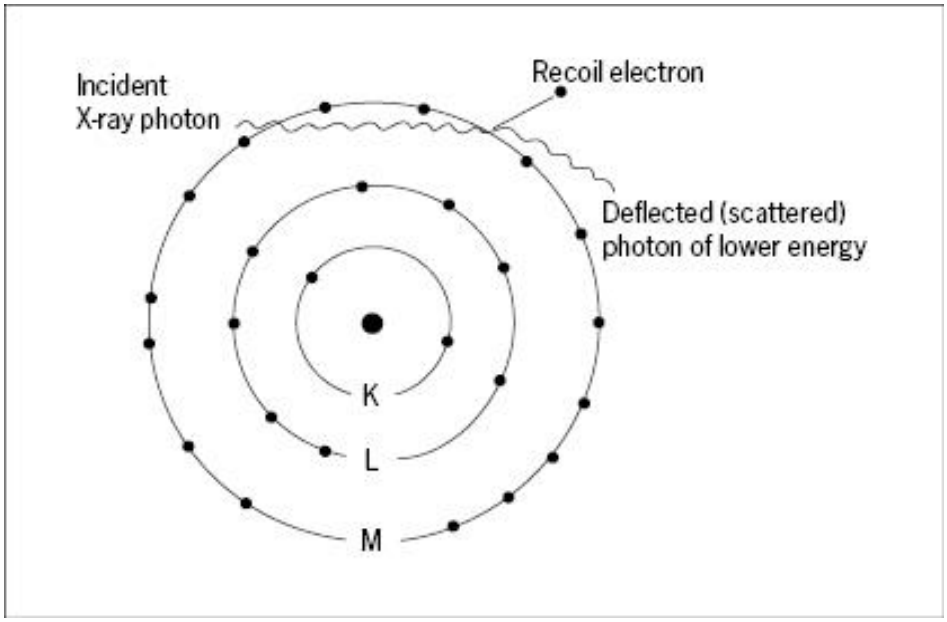


Figure I.7 : Inelastic (Compton) scatter [15]

3.3 Photoelectric Effect

The photoelectric effect occurs when an X-ray photon is completely absorbed by an atom, transferring all its energy to an inner-shell electron, which is then ejected from the atom. This leads to ionization of the atom.

This effect is the main mechanism of X-ray absorption, especially in materials with high atomic number and at lower photon energies. The atom may later emit characteristic X-rays to return to a stable state**[14]**. Figure I.8 depicts the photoelectric interaction.

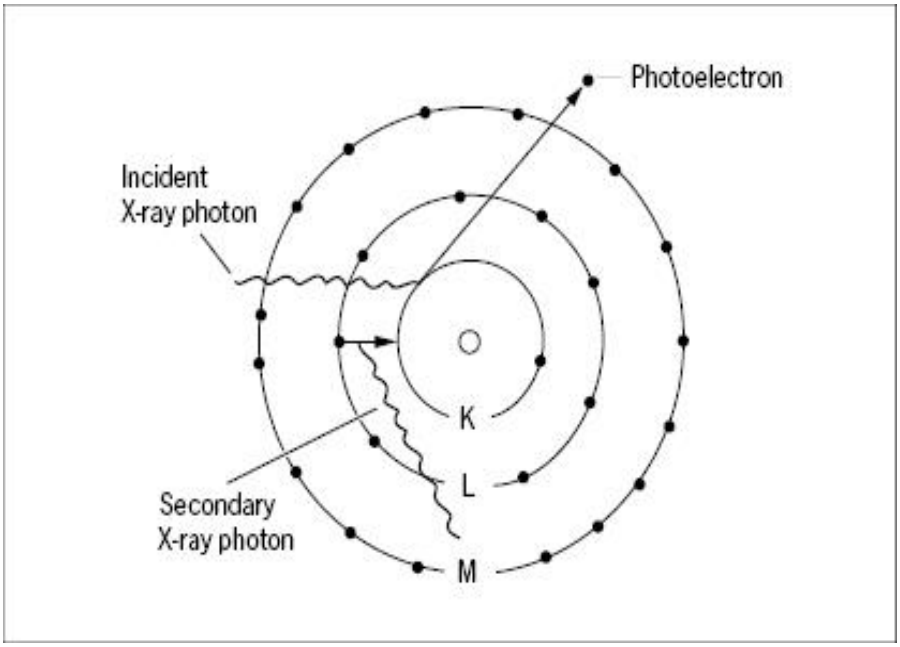


Figure I.8 : The photoelectric interaction [15]

3.4 Pair production

Pair production occurs when the energy of an X-ray photon is higher than 1.02 MeV. In this process, the photon is converted into an electron–positron pair. The positron is unstable and quickly annihilates with an electron, producing two photons. This interaction is mainly observed at very high photon energies and in high atomic number materials. It is not significant in diagnostic X-ray imaging because the energies used in CT are much lower than the threshold **[14]**. Figure I.9 describe pair production.

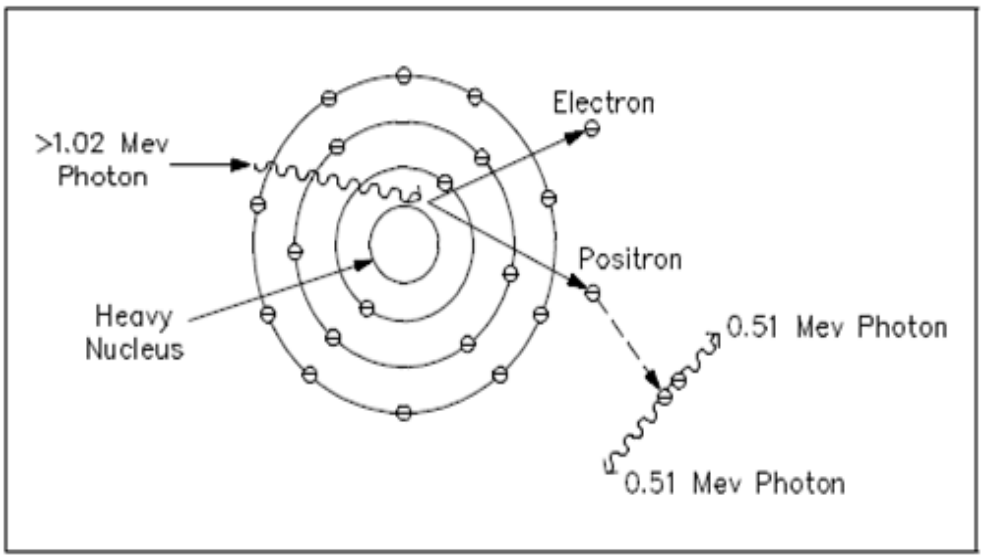


Figure I.9 : Pair Production [16]

The following figure illustrates the dominant domains of photon–matter interaction mechanisms as a function of photon energy and the atomic number of the medium. Figure I.10

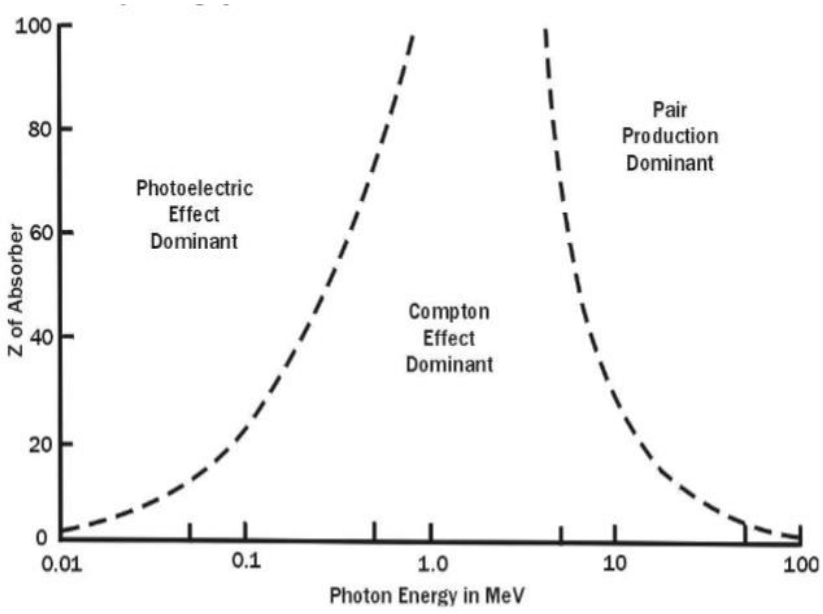


Figure I.10 : Photon interaction with matter diagram[14]

4 Dosimetry

Radiation dosimetry is the determination of the absorbed dose or dose rate resulting from the interaction of ionizing radiation with matter. This can be done either by measurement or by calculation. It is used to evaluate the amount of radiation absorbed in a material or tissue as a result of this interaction [17].

4.1 Absorbed Dose

Absorbed dose is a fundamental physical quantity that describes the energy deposited in tissue or material due to ionizing radiation. It is measured in gray (Gy), where 1 gray equals 1 joule per kilogram. It is used to represent the average energy deposited per unit mass of a material or tissue.

$$D = \frac{E}{m} \qquad \text{I. 5}$$

Where:

- D: absorbed dose (Gy)
- E: absorbed energy (J)
- m: mass of the material (kg) **[18].**

4.2 Equivalent Dose

Different types of ionizing radiation may produce different levels of stochastic effects even when the absorbed dose is the same. Therefore, the concept of equivalent dose (W_T) is used for a specific organ or tissue (T).

It is defined as:

$$H_T = \sum W_R \,.\, D_{T,R} \qquad \text{I. 6}$$

Where:

H_T: Equivalent dose (Sv)

W_R : Radiation weighting factor associated with the type of radiation, and the summation is taken over all radiation types.

$D_{T,R}$: Absorbed dose in the tissue (Gy)

For diagnostic X-rays, W_R=1

Therefore, H_T=D_T

The **sievert (Sv)** is the SI unit used to express equivalent dose and effective dose, which quantify the biological effects of ionizing radiation. Unlike the gray (Gy), which represents the absorbed energy per unit mass, the **sievert** accounts for both the type of radiation and the radiosensitivity of the exposed tissue **[10].**

Table I.2 : Tissue weighting factors **(W_R)** for different types of radiation**[18]**

Type of radiation	W_R
Photons	1
Electrons	1
Neutrons (E < 10 keV)	5
Neutrons (10 keV < E < 2 MeV)	20
Protons	5
Alpha particles (α)	20

4.3 Effective Dose

Effective dose is a quantity used to assess the overall radiation impact on the human body, since the risk of radiation varies from one organ to another. It is calculated by summing the product of the equivalent dose in each organ and its corresponding tissue weighting factor.

$$E = \sum W_T \, . H_T \qquad \text{I. 7}$$

Where:

- E: Effective dose (Sv)
- H_T: Equivalent dose in the organ or tissue
- W_T: Tissue weighting factor (the sum of all factors equals 1)

The unit of effective dose is the sievert (Sv). which is the same unit used for equivalent dose **[10]**

Table I. 3 Publication 103 (ICRP, 2007a) tissue weighting factors **[19]**

Tissue / organ group	**(W_T)**
Bone marrow, colon, lung, stomach, breast, remainder tissues	0.12
Gonads	0.08
Bladder, oesophagus, liver, thyroid	0.04
Bone surface, brain, salivary glands, skin	0.01
Total	**1.00**

4.4 Importance of dosemetry

Dosimetry plays an important role in radiation protection by providing a quantitative way to measure and monitor the radiation dose received by tissues or patients. It helps control exposure levels and ensures the safe use of ionizing radiation in different applications. It is also essential for dose optimization, supporting the ALARA principle of keeping radiation exposure as low as reasonably achievable**[19]**.

5 Medical Imaging Systems Using X-rays

X-rays are widely used in medicine for examining internal organs and diagnosing many diseases. With the development of medical imaging technologies, they provide clearer and more accurate images, which helps improve medical diagnosis and patient follow-up. In general, the applications of X-rays in medicine are divided into diagnostic and therapeutic uses**[10].**

5.1 Diagnostic Applications

5.1.1 Conventional Radiography

Conventional radiography is a commonly used X-ray technique in medicine for imaging internal structures of the body. It allows visualization of organs and tissues, where bones appear lighter due to their high density, while soft tissues appear darker. It is mainly used in the detection of fractures and certain pathological conditions **[20]**.

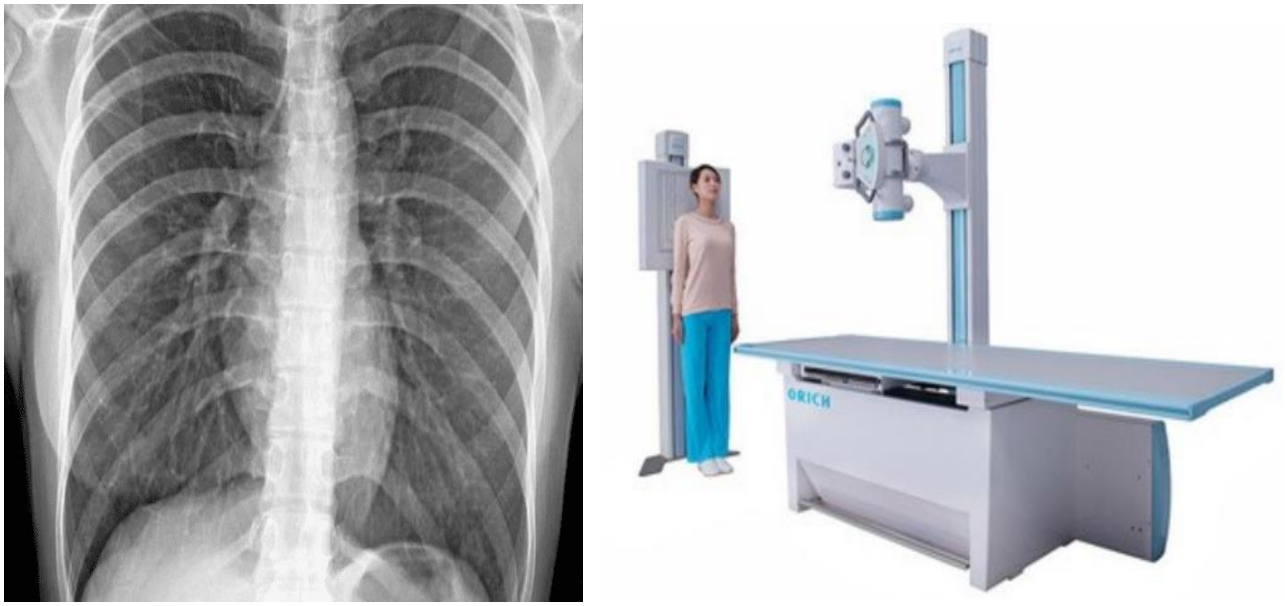


Figure I.11: Chest examination using conventional radiography **[21]**

5.1.2 Fluoroscopy

Fluoroscopy is an X-ray technique that produces real-time moving images of internal organs using a low-dose X-ray beam. It helps in observing organ motion and is widely used during medical procedures such as catheter insertion and biopsies. Contrast agents may be added to enhance image quality **[20]**.



Figure I.12: Fluoroscopy machine

5.1.3 Mammography

Mammography is a low-dose X-ray technique designed for breast tissue examination and early detection of abnormalities such as breast cancer. The use of digital systems has improved image clarity and reduced examination time compared to traditional methods**[20]**.



Figure I.13: Mammography Machine**[22]**

5.1.4 Angiography

Angiography is an imaging technique that uses X-rays to visualize blood vessels and diagnose diseases of the circulatory system. It is performed after injecting a contrast agent to make the vessels more clearly visible. It is used to detect blockages, aneurysms, and certain cardiac and vascular diseases. It can also sometimes be combined with therapeutic procedures such as angioplasty or stent placement **[20]**.



Figure I.14: Angiography Machine

5.1.5 Computed Tomography (CT)

Computed tomography is a modern X-ray–based imaging technique used to obtain detailed cross-sectional images of the human body. During the scan, the patient lies on a moving table that passes through a rotating gantry, while the X-ray tube rotates around the body to acquire images from different angles. The acquired data are processed by a computer to generate high-resolution 2D and 3D images**[20].**

This technique is widely used to diagnose various conditions such as fractures, internal bleeding, tumors, and traumatic injuries. Because of its speed and accuracy, CT has become an essential tool in medical imaging, especially in emergency cases **[20]**. Figure I.15 illustrates a computed tomography (CT) scanner.



Figure I.5 : Computed Tomography (CT) Scanner

5.2 Therapeutic Applications

5.2.1 Radiotherapy

In addition to its diagnostic role, X-rays are also used in the treatment of certain types of cancer through radiotherapy. Carefully controlled high doses are directed toward cancer cells in order to damage their DNA, leading to cell death or inhibition of their growth. This treatment is performed with high precision to minimize the impact on surrounding healthy tissues as much as possible**[20].**



Figure I.16: Radiotherapy Unit**[23]**

6 Radiation Protection

ICRP Publication 103 is the main international reference in radiation protection. It provides a framework for controlling exposure to ionizing radiation and protecting people from its harmful effects. Published in 2007, it is widely used in medical imaging, including X-ray and CT applications**[24]**.

6.1 Basic Principles of Radiation Protection

Radiation protection is based on three main principles:

6.1.1 Justification

any use of radiation must provide a real medical benefit that outweighs the potential risk.

6.1.2 Optimization (ALARA)

radiation doses should be kept as low as reasonably achievable without compromising diagnostic image quality.

6.1.3 Dose limits

set maximum permitted doses for workers and the public, but do not apply to patients since their exposure serves a direct medical purpose. According to ICRP recommendations, the occupational dose limit is 20 mSv per year averaged over five years, while the public limit is 1 mSv per year**[25]**.

6.2 Diagnostic Reference Levels (DRLs)

Diagnostic Reference Levels (DRLs) are reference values used to guide dose optimization in medical imaging. They help identify cases where patient doses are higher than necessary and support the improvement of imaging protocols without reducing diagnostic quality. In CT examinations, DRLs are particularly important as they help balance radiation dose and image quality, which is the main focus of this work **[25].**

7 Conclusion

Understanding the fundamental principles of ionizing radiation is essential for explaining the operation of medical imaging systems. Knowledge of X-rays, including their production, physical properties, and interactions with matter, provides the scientific basis for image formation and the factors that influence image quality. Furthermore, an understanding of radiation dosimetry and radiation protection principles highlights the importance of optimizing radiation exposure to ensure patient safety while maintaining diagnostic performance.

Among the various medical imaging modalities that use X-rays, Computed Tomography (CT) plays a particularly important role because of its high diagnostic accuracy and widespread clinical use. However, CT examinations are associated with relatively higher radiation doses than most conventional imaging techniques, making dose optimization a major concern in medical physics.

The concepts presented in this chapter provide the theoretical foundation for the remainder of this thesis. The following chapters focus on Computed Tomography (CT), examining the relationship between radiation dose and image quality and evaluating strategies for optimizing this balance while preserving diagnostic reliability.

Chapter II

Materials and Methods

1 Introduction

This chapter describes the materials and methods used to investigate the relationship between radiation dose and image quality in computed tomography (CT) examinations. The study was conducted in the Computed Tomography Unit of the Medical Imaging Department at Ibn Rochd University Hospital, Annaba, using a 64-slice FUJIFILM SCENARIA View CT scanner.

A quantitative descriptive study design was adopted, based on data obtained from routine three-phase thoraco-abdomino-pelvic (TAP) CT examinations, with the analysis focused on the portal venous phase. The examinations were performed according to the department's standard clinical protocols.

This chapter outlines the study design, patient selection criteria, CT acquisition protocols, radiation dose indicators, image quality assessment methods, and data analysis procedures. Together, these methods provide a reliable framework for evaluating the relationship between radiation dose and diagnostic image quality.

2 Presentation of the Medical Imaging Department

The practical internship took place at the Medical Imaging Department of Ibn Rochd University Hospital (CHU) in Annaba. This university hospital provides diagnostic, therapeutic, and training services across different medical and paramedical specialties.

Several imaging modalities are available in the department, including conventional radiography, computed tomography (CT), magnetic resonance imaging (MRI), ultrasonography, and other diagnostic examinations. The hospital has two CT scanners: one dedicated to the radiology department and another used in the emergency department.

The CT unit receives both emergency and scheduled patients, including inpatients and outpatients, for a wide range of diagnostic examinations. Different types of CT scans are performed, such as head, chest, and abdominal imaging. Workflow is well organized to ensure smooth patient management from reception through to image acquisition.

Medical activities are carried out by a multidisciplinary team composed of radiologists, resident doctors, interns, and medical imaging technologists. Close coordination is maintained between radiologists, technologists, and other healthcare staff. The department also collaborates with medical physicists from the Cancer Control Center (CAC), who conduct regular visits related to radiation protection and safety.

Through high-quality cross-sectional imaging, the CT department plays an important role in the diagnosis and follow-up of many medical conditions.

3 CT Scanner Used in the Study

This study was carried out using a computed tomography (CT) scanner, SCENARIA View Whole Body X-ray CT System, manufactured by FUJIFILM Corporation (Japan). It is a multi-slice CT (MDCT) system with 64 slices and operates using helical scanning technology. The system is equipped with an automatic injector system for contrast media. Figure II.1



Figure II.1 : CT scanner used for this study at Ibn Rochd University Hospital, Annaba

4 CT Principle

Computed Tomography (CT) is a medical imaging technique that combines X-ray beams and computer processing to produce cross-sectional images of the body.

During scanning, X-ray beams rotate around the patient while detectors collect the transmitted radiation from multiple angles. The signals are then converted into electrical data and reconstructed into detailed images of different anatomical structures.

Image formation relies on X-ray attenuation. This value changes based on tissue density, atomic number, and photon energy, which creates visible differences in image contrast.

CT images appear in grayscale. Bone and other dense structures show up white, while soft tissues and fat appear darker.

Each pixel represents an attenuation value measured in Hounsfield Units (HU), which help identify and differentiate various tissue types.

The whole process runs through three steps: data acquisition, image reconstruction, and image display **[26]**.

5 CT Scanner Components

Computed Tomography (CT) is based on the use of X-ray beams produced by a rotating tube to generate cross-sectional images of the body. This system consists of several interconnected components responsible for data acquisition, processing, and image display.

A CT scanner includes the generator, the gantry, the X-ray tube, detectors, radiation shielding elements, the patient table, the image processor, and the control console.

5.1 Generator

The generator provides the electrical power required to produce X-rays. It supplies a high voltage to accelerate electrons and a low voltage to heat the filament, ensuring continuous electron emission.

5.2 Gantry

The gantry is the main rotating structure of the CT scanner. It contains the X-ray tube, detectors, and shielding components, and rotates around the patient during image acquisition.

5.3 X-ray Tube

The X-ray tube converts electrical energy into X-ray photons. Electrons are emitted from a heated filament and accelerated toward the anode. When they strike the focal spot, X-rays are produced through characteristic radiation and Bremsstrahlung. The focal spot size can be adjusted depending on the required image resolution. About 99% of the energy is converted into heat, so an oil-based cooling system is used to dissipate heat and provide electrical insulation.

5.4 Detectors

Detectors receive the transmitted X-rays after they pass through the body and convert them into electrical signals used for image reconstruction.

5.5 Radiation Shielding Elements

Shielding elements are used to reduce the effects of scattered radiation, which can degrade image quality and increase noise. These include collimators, which absorb low-energy photons and help improve image quality while reducing radiation exposure.

5.6 Patient Table

The patient table moves through the gantry during scanning, allowing the acquisition of sequential cross-sectional images and defining the concept of pitch.

5.7 Image Processor

The image processor receives signals from the detectors and converts them into digital data representing the structure of the scanned body. These data are then processed using mathematical algorithms and reconstruction techniques to produce clear, displayable images.

5.8 Control Console

The control console displays images on an electronic screen composed of a matrix of pixels, where each pixel represents a two-dimensional projection of a three-dimensional volume known as a voxel. Each pixel is assigned a numerical value representing X-ray attenuation based on the Hounsfield Unit (HU) scale, calculated using the following relation:

$$\mathrm{HU} = 1000 \times \frac{\mu_{\mathrm{tissue}} - \mu_{\mathrm{water}}}{\mu_{\mathrm{water}}} \qquad \text{II. 1}$$

Where:

- μ_{tissue}: linear attenuation coefficient of the tissue
- μ_{water}: linear attenuation coefficient of water (reference value)

Higher HU values correspond to brighter pixels. Image display can also be adjusted using Window Width and Window Level to optimize contrast and brightness according to diagnostic needs**[27]**. Figure II.2 present Some components of the CT scanner used in this study.



Figure II.2 : Some components of the CT scanner used in this study

6 Methodology of the Study

6.1 Study Type

This study adopts a quantitative descriptive analytical design, with the aim of exploring the relationship between radiation dose and image quality in CT examinations of the chest, abdomen, and pelvis (TAP), particularly during the portal venous phase.

Data were obtained from routine CT examinations carried out under real clinical conditions, without any modification to the existing imaging protocols.

Due to its high frequency in daily practice within the medical imaging department, the TAP examination was selected among the available CT studies. It is especially common for patients followed at the Cancer Control Center (CAC), making it an appropriate choice for assessing dose–image quality relationships in a realistic clinical environment.

6.2 Study Sample and Characteristics

The study included a sample of 12 patients, equally distributed between 6 males and 6 females, who underwent the same CT examinations during the internship period. Cases were

randomly selected from routine examinations available during the study period, with exclusion applied only when data were incomplete.

Inclusion criteria were defined as follows: patients who underwent a TAP CT scan in the portal venous phase, availability of complete protocol information, full dose data (CTDIvol and DLP), and image quality sufficient for both assessment and statistical analysis.

Certain cases were excluded when specific conditions were not met, including missing dose or protocol data, non-diagnostic images due to significant motion artifacts, examinations performed outside the portal venous phase protocol, and patients with metallic implants causing relevant image distortion. The demographic characteristics of the patients are presented in the Table II.1.

Table II.1: Demographic Characteristics of the Patients

Patient Number	Sex	Age (years)	Kev
1	Male	28	120
2	Male	60	120
3	Male	77	120
4	Male	17	120
5	Male	60	120
6	Male	55	120
7	Female	49	120
8	Female	57	120
9	Female	58	120
10	Female	57	120
11	Female	53	120
12	Female	42	120

6.3 Study Conditions

This study was conducted during a practical internship period extending from early March to 9 April, within the medical imaging department and limited to working days only, excluding weekends.

The department operates using an Automatic Exposure Control (AEC) system, with no adjustments made to the scanner settings by the researcher. The role was limited to entering

basic patient information such as name, age, and sex, while the system automatically managed the remaining acquisition parameters.

Data collection was carried out through the CT scanner console and the protocol system, covering the entire examination process from setup to completion. This included acquisition parameters, dose indicators, and image quality metrics.

For data processing, Microsoft Excel was used to organize the dataset and generate tables and graphs, due to its simplicity and suitability for basic statistical analysis.

7 Triphasic CT Protocol for Thoraco-Abdomino-Pelvic Imaging

7.1 Patient Preparation for a Triphasic TAP CT Examination

Proper patient preparation is essential to ensure patient safety and to obtain high-quality diagnostic images during a **triphasic thoraco-abdomino-pelvic (TAP) CT** examination. This examination includes several consecutive imaging phases, namely the non-contrast phase, arterial phase, portal venous phase, and, when required, a delayed phase. Because multiple image acquisitions are performed during the same examination, the patient must remain still and follow the breathing instructions given by the radiographer. Good preparation helps reduce motion artifacts and improves the quality of the images obtained.

7.2 Before the Examination

Before the examination, several routine steps are performed to ensure patient safety and obtain high-quality images:

- Patient identification: The patient's identity is confirmed using their full name and date of birth. Pregnancy status is checked in women of childbearing age.
- Medical assessment: A brief medical history is taken, including previous allergic reactions to iodinated contrast media, asthma, and other significant allergies.
- Renal function evaluation: Recent serum creatinine and, when available, the estimated glomerular filtration rate (eGFR) are reviewed before contrast administration.
- Medication review: Current medications are checked, especially Metformin in diabetic patients. Temporary discontinuation may be recommended according to medical advice.
- Intravenous access: A peripheral intravenous (IV) cannula is inserted to allow contrast injection during the examination.
- Removal of metallic objects: The patient is asked to remove jewelry, belts, and other removable metallic objects to reduce image artifacts.

- Patient instructions: The procedure, including contrast injection and breathing instructions, is explained to help the patient remain calm and cooperative during the scan.

7.3 Special Precautions in Certain Cases

Some patients need extra precautions depending on their medical condition. For example, patients with a history of allergy or asthma may receive premedication before the examination. This is mainly done as a preventive measure to reduce the risk of contrast reaction. In patients with renal impairment, the use of contrast media is carefully evaluated. Sometimes the dose is reduced or completely avoided depending on the situation. Hydration is recommended when possible, and kidney function is checked before and after the scan.

7.4 Patient Positioning During the Examination

Patient positioning is a key factor for obtaining clear and reliable images. The patient lies in a supine position, usually head-first into the scanner. Both arms are raised above the head. This helps reduce artifacts, especially in the chest and abdomen, and improves image quality.

The patient is carefully centered inside the CT gantry to ensure full coverage from the thorax to the pelvis. A scout (topogram) image is first acquired to define the scan range and ensure correct patient positioning. It is very important that the patient remains still during the scan, since several phases are acquired one after another. In some cases, especially with children or uncooperative patients, immobilization may be necessary.

An automatic injector is connected to the IV line to deliver contrast material according to a precise timing protocol adapted to the different imaging phases. The patient positioning and the use of the automatic contrast injector during the triphasic TAP CT examination are illustrated in Figures II.3 and II.4.



Figure II. 3 : CT scout (topogram) image for scan range planning



Figure II.4 : Patient positioning during a TAP CT examination

7.5 Special Cases

In some situations, such as children, elderly patients, or uncooperative patients, a companion may be allowed in the scanning room. This helps reassure the patient and improves cooperation during the scan.

However, the companion must wear protective equipment, including a lead apron and thyroid shield, to reduce radiation exposure.

7.6 After the Examination

After the scan, the IV line is removed once it is no longer needed, and the injection site is checked for any local complications.

If the patient is stable, they can leave the department. In some cases, drinking water is recommended to help eliminate the contrast agent such as Iohexol through the kidneys.

A short observation period may be done after contrast injection to detect any early allergic reaction. The patient is also advised to report any delayed symptoms, such as skin rash or breathing difficulties.

8 Contrast Media

Iodinated contrast media are commonly used in CT scans to improve the visualization of blood vessels and soft tissues by increasing X-ray attenuation, which enhances image contrast.

These agents are given intravenously, usually with automatic injectors to ensure a controlled and accurate injection. After injection, the contrast first stays within the blood vessels during the initial phase, then gradually spreads into the surrounding extracellular interstitial space.

The level of contrast enhancement depends on several factors, including the properties of the contrast agent, the injection protocol, the timing of image acquisition, and the CT scanning parameters and technique used **[28].**



Figure II.5 : Contrast media used during the CT examination

9 Imaging Phases of a Multiphase TAP CT Examination

9.1 Phases of a Triphasic TAP CT Examination

After patient preparation and positioning in the CT scanner, image acquisition begins. A Triphasic TAP CT study is typically performed through a sequence of phases: non-contrast, arterial, portal venous, and occasionally delayed imaging, depending on the clinical indication.

9.1.1 Non-Contrast Phase

No contrast medium is administered in this phase. It serves as a baseline for evaluating abdominal structures before enhancement. Calcifications and urinary tract stones, such as renal or ureteral calculi, are better appreciated at this stage. The same applies to vascular calcifications, which may become less conspicuous after contrast injection **[29]**.

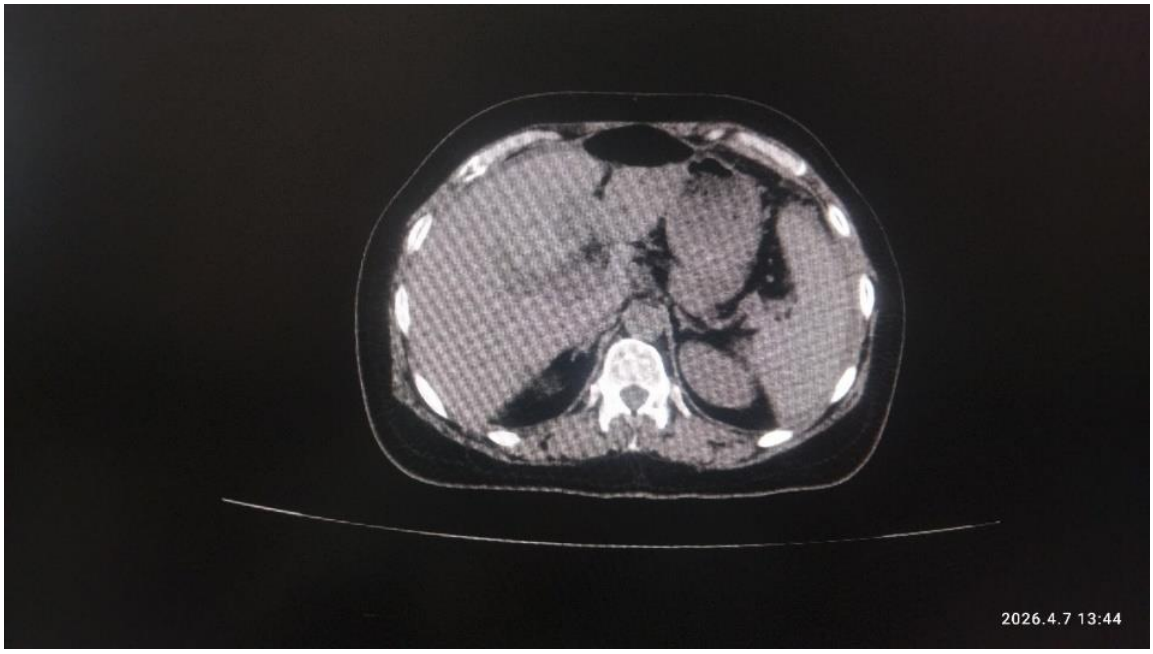


Figure II.6 : Liver CT image in the non-contrast phase

9.1.2 Arterial Phase

- **Early Arterial Phase**

Acquired seconds after contrast injection, this phase captures the rapid arterial enhancement. It is mainly used to assess arterial anatomy and identify vascular abnormalities, including dissection **[28]**.

- **Late Arterial Phase**

A short delay follows, typically 15–20 seconds. Solid organs begin to enhance more distinctly, improving lesion detection in highly vascular structures such as the liver, spleen, and kidneys **[29; 30]**.



Figure II.7 : Liver CT image in the arterial phase

9.1.3 Portal Venous Phase

This phase is obtained approximately 60–80 seconds after contrast administration. It represents a key stage in abdominal CT imaging. At this point, contrast is predominantly within the venous circulation, resulting in a more homogeneous enhancement of abdominal organs. It is particularly valuable for detecting hypovascular liver lesions and evaluating conditions such as portal hypertension **[28]**.



Figure II.8 : Liver CT image in the portal venous phase

9.1.4 Delayed Phase

Performed 6–10 minutes after injection, this phase reflects the excretory stage of contrast distribution. The agent is gradually cleared through the kidneys. It is useful for urinary tract assessment and for characterizing liver lesions based on their washout behavior, helping to differentiate benign from malignant findings [28].

9.2 Contrast Injection Considerations

Proper contrast administration is essential for obtaining optimal image enhancement during a multiphase TAP CT examination. The volume and injection rate of the iodinated contrast medium are adjusted according to the patient's body weight, clinical indication, and the examination protocol.

An appropriate peripheral intravenous (IV) cannula is selected to ensure safe administration at the required flow rate. Larger cannulas allow higher injection rates, which are often necessary for arterial phase imaging.

Automatic power injectors are routinely used because they provide accurate injection timing, constant flow rates, and better synchronization with image acquisition. Manual injection is reserved for selected cases when the use of an automatic injector is not possible **[30]** .

10 Radiation Dose Indicators

Radiation dose indicators are essential for evaluating and monitoring patient radiation exposure during CT examinations. The CT scanner automatically calculates these indicators for each examination. In this study, the dose data were obtained from the scanner console using the post-scan Dose Report. The recorded parameters included the Computed Tomography Dose Index volume (CTDIvol) and the Dose-Length Product (DLP), which are commonly used to estimate radiation output during CT imaging. Figure II.9 shows an example of the CT Dose Report.

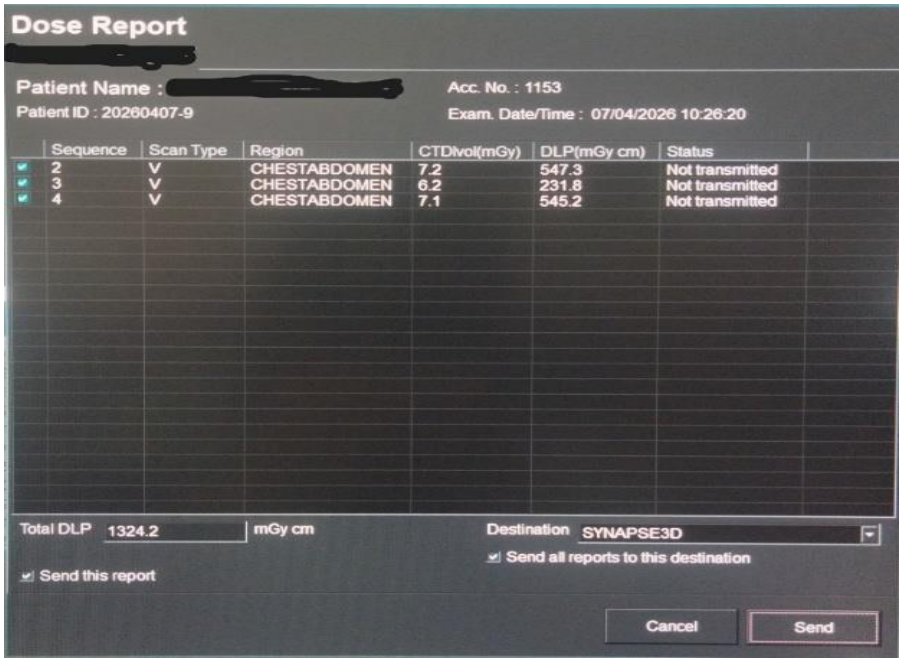


Figure II.9 : CT dose report of the examination

10.1 Computed Tomography Dose Index Volume (CTDIvol)

The volume CT dose index (CTDIvol) reflects the radiation intensity within the scanned slice. It is calculated using measurements from a standardized phantom (16 or 32 cm) and the scanning parameters. However, it does not represent the actual dose absorbed by the patient.

$$\mathrm{CTDI_{vol}} = \frac{\mathrm{CTDI_w}}{\mathrm{Pitch}} \qquad \text{II. 2}$$

Where:

- $CTDI_w$: Weighted CT dose index
- $Pitch$: Table movement per rotation divided by beam width

10.2 Dose-Length Product (DLP)

The dose–length product (DLP) is a measure of the total radiation exposure during a CT examination. It is calculated by multiplying CTDIvol by the scanned length. It is used to estimate the overall patient dose and the effective dose related to radiation risk.

$$\mathrm{DLP} = \mathrm{CTDI_{vol}} \times \mathrm{Scan\ Length} \qquad \text{II. 3}$$

Where:

- DLP : Dose–Length Product
- $CTDI_{vol}$: Volume CT Dose Index
- Scan Length: length of the scanned region

10.3 Effective Dose (E)

The effective dose represents the overall biological effect of radiation on the human body. It is used to compare different types of imaging examinations.

$$\mathrm{E} = \mathrm{DLP} \times \mathrm{K} \qquad \text{II. 4}$$

Where:

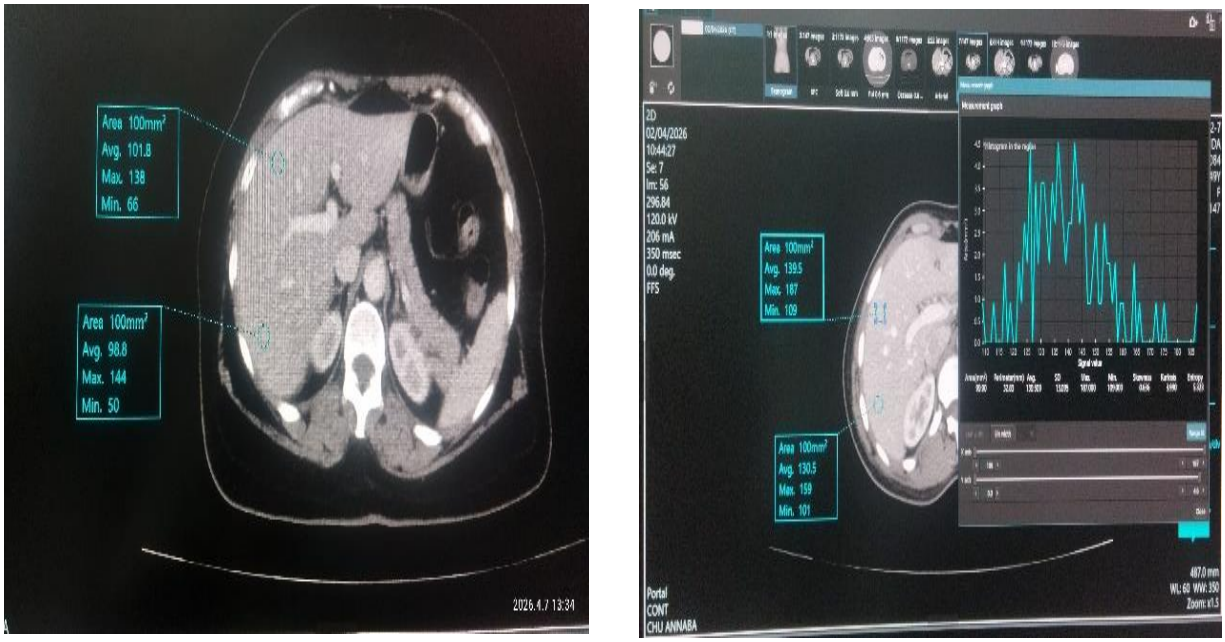
- **E** : Effective dose
- **DLP** : Dose–Length Product
- **k**: Conversion factor depending on the scanned anatomical region (e.g., chest or abdomen) **[31]**.

11 Image Quality Assessment

Image quality assessment was performed using images acquired during the portal venous phase. The liver level was selected in consultation with an experienced radiologist from the same department. For all patients, the same anatomical slice, located immediately before the portal vein bifurcation, was used to ensure measurement consistency and reduce inter-patient variability.

Two circular regions of interest (ROIs), each with an area of approximately 100 mm², were placed in homogeneous liver parenchyma on the selected slice. One ROI was positioned above the portal vein and the other below it, while carefully avoiding blood vessels, focal lesions, and heterogeneous areas to ensure accurate and reproducible measurements.

For each ROI, the mean attenuation value (Mean/AVG) and the standard deviation (SD) were recorded. These measurements were then used to calculate the objective image quality parameters, including image noise, signal-to-noise ratio (SNR), and contrast-to-noise ratio (CNR). The ROI placement method is illustrated in Figure II.10.



10**Figure II.11** : Methodology for region of interest (ROI) placement and liver image analysis in the portal venous phase

11.1Fundamental Concepts of Image Quality in CT

Image quality in computed tomography (CT) refers to the ability of the imaging system to produce images that provide sufficient diagnostic information to accurately answer the clinical question while minimizing patient radiation exposure in accordance with the ALARA (As Low As Reasonably Achievable) principle. Achieving optimal image quality requires an appropriate balance between image clarity and radiation dose, ensuring that the images are diagnostically acceptable without unnecessary patient exposure.

Image quality is influenced by several interrelated factors, including spatial resolution, contrast resolution, image noise, and image artifacts. These parameters determine the visibility of anatomical structures and pathological findings and are therefore essential for accurate

diagnosis. Optimizing CT protocols aims to achieve the best possible compromise between image quality and radiation dose according to the clinical indication **[32]**.

11.1.1 Spatial resolution

Spatial resolution is the ability of a CT imaging system to distinguish two closely adjacent structures as separate objects within an image. It determines the level of anatomical detail that can be visualized and plays a critical role in detecting small lesions and fine anatomical structures.

Spatial resolution is commonly expressed in line pairs per centimeter (lp/cm) and is quantitatively evaluated using the Modulation Transfer Function (MTF), which describes the system's ability to reproduce image details at different spatial frequencies. Several factors influence spatial resolution, including detector size, focal spot size, pixel size, reconstruction matrix, slice thickness, and reconstruction kernel. While improving spatial resolution enhances the visibility of fine details, it may also increase image noise, requiring an appropriate balance between image quality and radiation dose **[33]**.

11.1.2 Contrast resolution

Contrast resolution is the ability of a CT imaging system to distinguish between tissues that have small differences in X-ray attenuation or signal intensity. It is particularly important for detecting low-contrast lesions, such as soft tissue abnormalities, where differences in attenuation are minimal.

Unlike spatial resolution, contrast resolution is highly influenced by image noise. As image noise increases, the ability to differentiate tissues with similar attenuation decreases. Contrast resolution can be improved by optimizing acquisition parameters such as tube voltage (kVp), tube current-time product (mAs), slice thickness, and reconstruction algorithms. The administration of iodinated contrast media also enhances tissue contrast by increasing attenuation differences between normal and pathological structures.

The contrast between two tissues can be expressed as:

$$\text{contrast} = |S_1 - S_2| \qquad \text{II. 5}$$

- S_1: signal intensity of the first tissue
- S_2:signal intensity of the second tissue **[34]**.

Although this equation represents the difference in signal intensity between two tissues, the actual contrast resolution depends on both image contrast and the level of image noise.

11.1.3 Noise

Noise in computed tomography (CT) images is any deviation or distortion that does not reflect the true anatomical structure of the image, and all unwanted signals within the image are considered part of this noise. It arises from variations in the signals during image reconstruction, leading to reduced accuracy and decreased visibility of fine details.

Image noise is commonly quantified by the standard deviation (σ) of CT numbers measured within a homogeneous region of interest (ROI):

$$\text{Noise} = \sigma \qquad \text{II. 6}$$

σ represents the dispersion or variation in signal values within the image **[35]**.

Image noise is inversely related to the number of detected X-ray photons. Therefore, increasing the radiation dose generally reduces image noise, whereas reducing dose increases noise, highlighting the importance of balancing radiation exposure and image quality.

11.1.4 Image artifacts

Image artifacts are artificial features appearing in CT images that do not correspond to the patient's actual anatomy. They result from limitations of the imaging system, patient-related factors, physical interactions of X-rays, or image reconstruction processes. Artifacts may degrade image quality, obscure anatomical structures, or simulate pathological findings, thereby reducing diagnostic confidence **[36]**.

11.2Quantitative Image Quality Metrics in CT

Image quality evaluation indicators in computed tomography (CT) are used to assess image clarity and its ability to accurately display anatomical details. Among the most important of these indicators are:

11.2.1 Signal-to-noise ratio (SNR)

Signal-to-noise ratio (SNR) is a measure used to evaluate image quality in computed tomography imaging. It represents the relationship between the useful signal within the image and the level of accompanying noise. The higher the SNR value, the better and clearer the image quality. The Signal-to-Noise Ratio is calculated as :

$$SNR = \frac{Signal}{Noise} \qquad II.7$$

- **Signal**: Useful signal originating from the imaged structure or tissue
- **Noise**: Unwanted fluctuations or disturbances in the image

Or

$$\text{SNR} = \frac{\mu}{\sigma} \qquad \text{II. 8}$$

Where:

- μ is the mean CT number (mean signal intensity) measured within a homogeneous region of interest (ROI).
- σ : is the standard deviation of the CT numbers within the same ROI and represents image noise.

SNR is influenced by several acquisition parameters, including tube current (mAs), tube voltage (kVp), slice thickness, reconstruction algorithm, and patient size. Increasing the radiation dose generally increases the number of detected photons, thereby reducing quantum noise and improving SNR. Conversely, reducing the radiation dose increases image noise and decreases SNR **[37]**.

11.2.2 Contrast-to-noise ratio (CNR)

Contrast-to-noise ratio (CNR) is a measure used to evaluate the ability of an image to distinguish between the object and the background in the presence of noise within the image.

The higher the CNR value, the clearer the differences between tissues become, whereas a lower value makes it more difficult to distinguish anatomical structures.

$$\mathrm{CNR} = \frac{|S_1 - S_2|}{\sigma_{\mathrm{noise}}} \qquad \text{II. 9}$$

S_1: Signal intensity of region 1

S_2: Signal intensity of region 2

σ_{noise}: Standard deviation of noise **[38]**.

CNR depends on both tissue contrast and image noise. Increasing the attenuation difference between tissues or reducing image noise results in higher CNR values. Consequently, CNR is widely used in CT optimization studies because it provides a more realistic assessment of lesion conspicuity than SNR alone.

11.2.3 Advanced Image Quality Metrics

In addition to Noise, SNR, and CNR, several advanced quantitative metrics have been developed to provide a more comprehensive assessment of CT image quality. These parameters are primarily used in imaging physics research, quality assurance, and the evaluation of new CT technologies.

Advanced metrics are used for detailed evaluation of image quality in computed tomography (CT), such as: The Modulation Transfer Function (MTF) describes the system's ability to reproduce image details at different spatial frequencies**[39]** while the Noise Power Spectrum (NPS) illustrates how noise is distributed across these frequencies **[40]** The Detective Quantum Efficiency (DQE) represents the overall efficiency of the imaging system in

producing useful image signal while accounting for noise **[41]**. The Figure of Merit (FOM) is used to assess the balance between image quality and radiation dose**[42].**

However, this study focuses on Noise, SNR, and CNR as practical metrics directly related to radiation dose optimization. Influence of CT Technical Parameters and Patient Factors on Image Quality and Radiation Dose.

11.3Influence of CT Technical Parameters and Patient Factors on Image Quality and Radiation Dose

Several technical parameters and patient-related factors influence both radiation dose and image quality in computed tomography (CT). Appropriate adjustment of these parameters is essential to obtain diagnostically acceptable images while maintaining radiation exposure as low as reasonably achievable (ALARA). Understanding the effect of each parameter enables the optimization of CT protocols according to the clinical indication and patient characteristics.

11.3.1 Tube Current- Time Product (mAs)

Tube current, or its product with scan time (mAs), is a technical parameter that controls the number of X-ray photons produced during a CT examination. Increasing mAs improves image quality and reduces image noise, but it also increases patient radiation dose. There is an approximately linear relationship between mAs and dose, meaning that any increase in mAs leads to a proportional increase in radiation dose. Most modern CT systems use Automatic Tube Current Modulation (Automatic Exposure Control) to optimize image quality while managing patient dose.

$$\text{mAs} = \text{mA} \times \text{Time} \qquad \text{II.10}$$

- mAs represents the total X-ray tube output.
- mA is the tube current.
- Time is the tube rotation time in (CT)

During the internship, it was observed that the CT scanner automatically adjusted mA according to patient body density and the examined region, increasing it in high-density areas and decreasing it in low-density areas to maintain image quality while controlling radiation dose.

11.3.2 Patient Positioning

Accurate patient positioning is an essential component of CT protocol optimization. Proper centering of the patient within the scanner gantry ensures optimal performance of the

bow-tie filter and Automatic Tube Current Modulation (ATCM), thereby improving image quality and reducing radiation dose.

A study by Li et al. (2006) reported that 95% of patients were not properly centered within the CT scanner gantry by the technologist. Although this may seem minor, incorrect positioning can significantly influence both image noise and surface dose.

Similarly, Habibzadeh et al. found that improper centering of phantoms within the scanner gantry increases surface dose by an average of 23% and image noise by 7%**[43]**.

11.3.3 Pitch

In spiral CT, pitch is defined as the ratio of table movement per rotation to beam collimation. Since the CT scanner used during the internship operated in spiral acquisition mode, pitch was an important acquisition parameter. A pitch lower than 1 indicates slice overlap, while a pitch greater than 1 indicates gaps between slices. A pitch equal to 1 corresponds to contiguous slices without overlap or gaps. Decreasing pitch increases overlap and sampling, resulting in a higher radiation dose.

11.3.4 Slice Thickness (dose-focused)

Slice thickness has an indirect effect on radiation dose. Decreasing slice thickness reduces the number of photons within each voxel and increases image noise, which requires a higher radiation dose to maintain image quality. Furthermore, the presence of automatic tube current modulation makes the relationship between slice thickness and radiation dose more complex, depending on the selected noise level.

11.3.5 Scan Range (Scan Length)

In CT examinations, the scan range should always be limited to the minimum required for diagnostic purposes. In some cases, such as thoraco-abdomino-pelvic (TAP) CT, the range is inherently extensive and cannot be significantly reduced. However, careful definition of scan boundaries remains essential to avoid unnecessary irradiation of non-targeted anatomical regions **[43].**

11.3.6 Tube Voltage (kVp)

Tube voltage (kVp) determines the peak energy of the X-ray beam and is one of the principal acquisition parameters affecting both radiation dose and image quality. Increasing kVp increases photon energy and beam penetration, allowing X-rays to pass more easily through dense anatomical structures. As a result, image noise generally decreases because more photons reach the detectors **[44]**.

11.3.7 Patient size (BMI, weight, and height)

Patient body size is an important determinant of both image quality and radiation dose in CT. Parameters such as body mass index (BMI), body weight, body height, and maximum body diameter reflect the amount of tissue that must be penetrated by the X-ray beam.

Therefore, the larger the body size, the higher the radiation dose required to obtain a diagnostically adequate image. The scanned region in CT affects the radiation dose, as it increases with a larger scan range and a greater number of body areas included, such as comparing a single-region scan to a multi-region scan (e.g., abdomen only versus abdomen combined with pelvis) **[45]**.

11.3.8 Age

Patient age is another important factor influencing CT protocol optimization. Children are considerably more radiosensitive than adults because their tissues contain rapidly dividing cells and they have a longer life expectancy during which radiation-induced effects may develop. Consequently, pediatric CT examinations require dedicated low-dose protocols specifically adapted to patient size and clinical indication **[46]**.

12 Dose Reduction and Radiation Protection in Computed Tomography (CT)

12.1 Modern Equipment Technologies

12.1.1 Automatic Exposure Control (AEC)

Automatic Exposure Control (AEC) is a CT technique that automatically adjusts the X-ray tube current (mA) based on differences in radiation attenuation inside the patient's body. The tube current is reduced in low-attenuation areas such as the lungs, and increased in high-attenuation regions such as the shoulders. This adjustment is applied continuously during scanning, as tissue attenuation changes with tube rotation and table movement along the body **[47]**.

12.1.2 Organ-Based Tube Current Modulation (OTCM)

Organ-Based Tube Current Modulation (OTCM) reduces the tube current (mA) during anterior projections of the X-ray tube rotation around the patient. The goal is to lower radiation dose to superficial sensitive organs such as the eyes, breasts, and thyroid. Studies have shown that this technique reduces dose to these organs, with only a slight increase in image noise in the affected regions, while maintaining acceptable diagnostic image quality**[48]**.

12.1.3 Image Quality Improvement at Low Doses

Model-Based Iterative Reconstruction (MBIR) algorithms are used to improve image quality at low radiation doses compared to the traditional Filtered Back Projection (FBP) method. Noise is reduced while anatomical details are preserved. Kataria et al. (2018) demonstrated in abdominal CT that dose reductions of 22–47% are achievable using ADMIRE 3, and 34–74% using ADMIRE 5, with only a limited effect on liver tissue clarity at the highest reconstruction strength **[49]**.

12.2 Radiation Protection Procedures

12.2.1 Use of Protective Devices for Sensitive Organs

Lead aprons and shielding devices are used during CT to reduce radiation dose to sensitive organs outside the scan field, such as the testes, ovaries, bladder, and colon. These organs may be exposed to scattered radiation during imaging. Shielding reduces unnecessary exposure without affecting diagnostic image quality, making it an essential component of the ALARA principle in medical imaging**[50].**

12.2.2 Limitation of Scan Range

Limiting the scan range is a key radiation protection measure in CT. The scan area is restricted to the anatomical region required by the clinical indication, reducing radiation exposure to uninvolved tissues and organs without compromising diagnostic value[51]. Studies have shown that reducing scan length decreases radiation dose while maintaining diagnostic accuracy when appropriate anatomical boundaries are selected[51] Over-scanning, however, increases patient dose without providing additional diagnostic information, which makes careful scan planning essential**[52]**.

12.2.3 Selection of the Appropriate Scanning Protocol

Selecting the right CT protocol is essential for balancing image quality with dose reduction. Protocol selection depends on factors such as patient size, examination type, and diagnostic requirements, with exposure parameters like kVp and mAs adjusted for each case. Protocols are individually adapted to ensure good diagnostic quality at the lowest possible dose, in line with the ALARA principle **[53]**.

12.2.4 Justification of Examination

Justification is one of the fundamental principles of radiation protection in medical imaging. Before any CT examination, it must be confirmed that the procedure is clinically necessary and that the expected diagnostic or therapeutic benefit outweighs the potential risk from radiation exposure. This principle applies to all patients, with particular attention to

sensitive groups such as children and pregnant women. Justification requires individual patient assessment by both the referring physician and the radiologist. Radiation-free or lower-dose imaging alternatives should also be considered when they can provide equivalent diagnostic information. This process helps avoid unnecessary or repeated examinations and minimizes radiation dose in accordance with the ALARA principle **[54]**.

12.2.5 Optimization

Optimization is a practical application of the ALARA principle. The aim is to reduce radiation dose to the lowest achievable level while maintaining the required diagnostic image quality. This is achieved by balancing diagnostic needs with dose reduction through improved scanning protocols and appropriate selection of imaging parameters based on patient condition and examination type, ensuring maximum medical benefit with minimum radiation exposure (IAEA) **[54].**

13 Impact of Image Quality on Diagnosis

Image quality in computed tomography (CT) has a direct impact on diagnostic accuracy, as it determines the level of anatomical detail visibility and the ability to distinguish fine structures. Improving image quality enhances the visualization of tissues and small lesions, thereby strengthening diagnostic performance. On the other hand, increased image noise leads to a reduction in the signal-to-noise ratio (SNR), resulting in the loss of fine image details. Spatial resolution and the reconstruction filters used also play a crucial role in determining image sharpness and the ability to separate different anatomical structures. Furthermore, imaging artifacts, such as those caused by patient motion or the presence of metallic objects, can degrade image quality and lead to interpretation errors. Image quality is also closely linked to radiation dose, which requires a careful balance between achieving high-quality images and minimizing patient radiation exposure **[55].**

14 Conclusion

This chapter presented the materials and methods used in the present study, including the clinical setting, the CT imaging system, patient selection criteria, data collection procedures, radiation dose assessment, and image quality evaluation. A standardized methodology was adopted throughout the study to ensure consistency and reproducibility. In particular, the use of predefined regions of interest (ROIs) for image quality analysis and standardized radiation dose indicators, namely CTDIvol and DLP, enabled reliable and objective data collection.

The methodology described in this chapter provides the foundation for the analysis presented in the following chapter. The results will focus on identifying the factors influencing radiation dose, evaluating the relationship between radiation dose and image quality, and assessing whether current clinical protocols achieve an appropriate balance between patient radiation protection and diagnostic performance. Ultimately, this study aims to support the optimization of CT examination protocols in accordance with the ALARA principle while maintaining adequate diagnostic image quality.

Chapter III

Results and Discussion

1 Introduction

This chapter presents and discusses the results obtained from the analysis of radiation dose and image quality in contrast-enhanced computed tomography (CT) examinations of the chest, abdomen, and pelvis (TAP CT) during the portal venous phase. Radiation dose was evaluated using the standard dosimetric indicators CTDIvol, DLP, and mAs, together with the demographic characteristics of the study population, including age and sex.

Image quality was assessed using objective quantitative parameters, namely image noise, signal-to-noise ratio (SNR), and contrast-to-noise ratio (CNR). The relationships between radiation dose and image quality were examined, while the influence of both technical and patient-related factors, particularly tube current, age, and sex, on the measured dose and image quality parameters was also investigated.

Furthermore, radiation dose levels in TAP CT during the portal venous phase were compared with those of contrast-enhanced brain CT to identify differences associated with the examination type and imaging protocol. The findings are discussed in the context of dose optimization and image quality, with reference to the ALARA (As Low As Reasonably Achievable) principle, to evaluate whether diagnostic image quality can be maintained while minimizing patient radiation exposure.

2 Radiation Dose Analysis

All patients included in this group underwent a contrast-enhanced computed tomography examination of the chest, abdomen, and pelvis (TAP CT) during the portal venous phase. Table III.1 presents the demographic characteristics of the study population (age and sex) together with the recorded radiation dose parameters, including CTDIvol, DLP, and mAs. A total of 12 patients were included, equally distributed between males and females, with ages ranging from 17 to 77 years. All examinations were performed using a constant tube voltage of 120 kVp. The CTDIvol values ranged from 6.4 to 8.9 mGy, the DLP values from 486.4 to 677.7 mGy·cm, and the mAs values from 81.9 to 112 mAs.

The variation in radiation dose among patients is mainly associated with differences in mAs and patient characteristics. Overall, the recorded dose values remained within the range commonly reported for routine adult TAP CT examinations and were consistent with international diagnostic reference levels (DRLs), indicating an appropriate balance between radiation dose and diagnostic image quality in accordance with the ALARA principle.

The relatively small variation observed in the radiation dose parameters (CTDIvol, DLP, and mAs) reflects the use of a standardized acquisition protocol for all patients. Since all examinations were performed using the same tube voltage (120 kVp) and the same imaging protocol during the portal venous phase, only limited variations in radiation dose were expected. These differences are mainly attributable to patient-related factors and automatic tube current modulation (ATCM), which adjusts the tube current according to the patient's attenuation while maintaining consistent image quality.

Table III.1 : Patient demographic characteristics and radiation dose parameters for TAP CT examinations in the portal venous phase

Patient Number	Sex	Age (years)	Kev	CTDIvol (mGy)	DLP (mGy·cm)	mAs (mA·s)
1	Male	28	120	7.1	511.5	87.1
2	Male	60	120	6.4	486.4	81.9
3	Male	77	120	8.9	602.2	112
4	Male	17	120	7.4	564.7	93.4
5	Male	60	120	7.1	545.2	89.6
6	Male	55	120	7.9	567	99.4
7	Female	49	120	7.6	577	94.9
8	Female	57	120	8.9	677.7	112
9	Female	58	120	8.7	630.5	105
10	Female	57	120	8.9	602.2	112
11	Female	53	120	8.8	674.2	110.6
12	Female	42	120	8.7	630.3	110.8

2.1 Effect of Age on Radiation Dose Accoeding to sex

2.1.1 CTDIvol

Figure III.1 illustrates the relationship between age and CTDIvol values according to sex in thoraco-abdomino-pelvic computed tomography (TAP CT) examinations performed during the portal venous phase. CTDIvol values ranged from (6.4 to 8.9 mGy) in males and from (7.6 to 8.9 mGy) in females, with substantial overlap between the two groups.

Visual inspection of the data showed no consistent increase or decrease in CTDIvol with age in either males or females. This observation is supported by the low coefficients of

determination (R^2 = 0.1468 for males and R^2 = 0.1403 for females), indicating that age explained only a small proportion of the variability in CTDIvol.

The relatively narrow range of CTDIvol values can be explained by the use of a standardized acquisition protocol, in which all examinations were performed using a tube voltage of 120 kVp. Therefore, the small variations observed are more likely related to tube current modulation (mAs) and individual patient characteristics than to age itself.

Overall, the findings suggest that no clear relationship was observed between age and CTDIvol in this study. Although female patients tended to present slightly higher CTDIvol values, the marked overlap between the two groups does not indicate a clear sex-related difference.

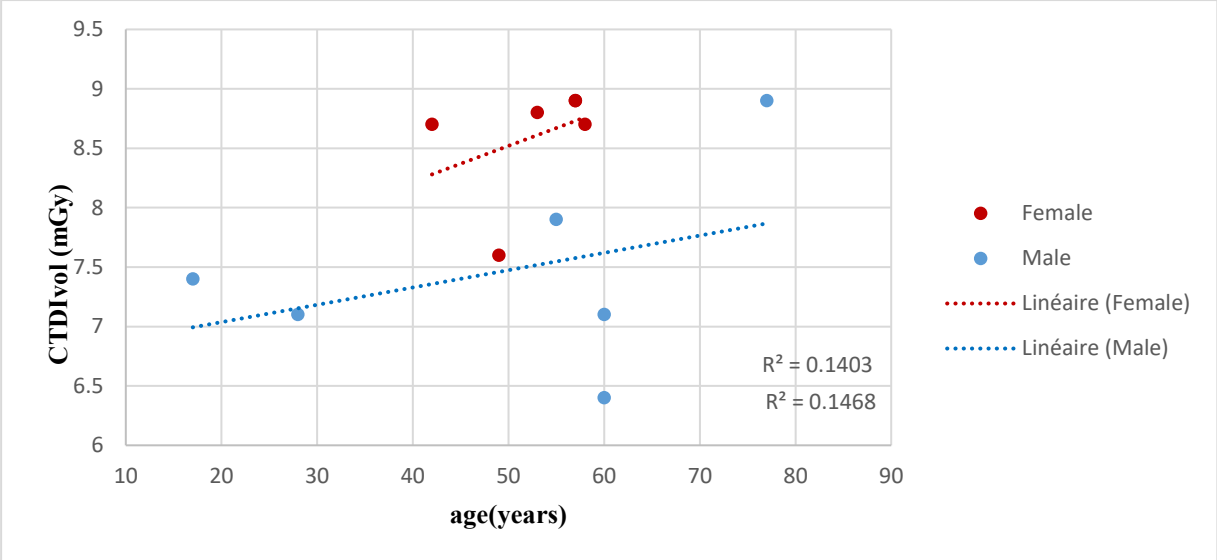


Figure III.1 : Relationship between Age and CTDIvol According to Sex in Portal Venous Phase TAP CT Examinations

Although CTDIvol values showed slight variations between male and female patients, the overall radiation dose remained relatively comparable, with considerable overlap between the two groups. This finding is expected because all examinations were performed using the same standardized TAP CT protocol at a fixed tube voltage of 120 kVp on the SCENARIA View CT system (FUJIFILM). In addition, the automatic exposure control (AEC) system adjusts the tube current according to patient attenuation to maintain consistent image quality while optimizing radiation dose. Consequently, only minor variations in CTDIvol were observed, reflecting

normal differences in patient characteristics rather than the effects of age or sex. The recorded dose values also remained within the range commonly reported for routine adult TAP CT examinations, indicating that the imaging protocol achieved an appropriate balance between diagnostic image quality and radiation protection in accordance with the ALARA principle

2.1.2 DLP

Figure III.2 illustrates the relationship between age and DLP values according to sex in thoraco-abdomino-pelvic computed tomography (TAP CT) examinations during the portal venous phase. DLP values ranged from 486.4 to 602.2 mGy·cm in males and from 577 to 677.7 mGy·cm in females, with considerable overlap between the two groups. No consistent increase or decrease in DLP with age was observed in either sex. This observation is supported by the low coefficients of determination (R^2 = 0.0614 for males and R^2 = 0.0577 for females), indicating that age explained only a very small proportion of the variability in DLP. As shown in Figures III.3 and III.4, all patients were examined using a standardized TAP CT protocol with a similar scan coverage. Consequently, the relatively small variation in DLP values is likely attributable to automatic exposure control (AEC), which adjusts the tube current according to patient attenuation, together with minor differences in patient morphology, rather than to age or sex. Overall, the results did not demonstrate a clear relationship between age and DLP values in either males or females, and the comparable DLP values indicate a consistent imaging protocol that maintained diagnostic image quality while optimizing radiation dose in accordance with the ALARA principle. These findings suggest that age and sex were not direct determinants of DLP in this study.

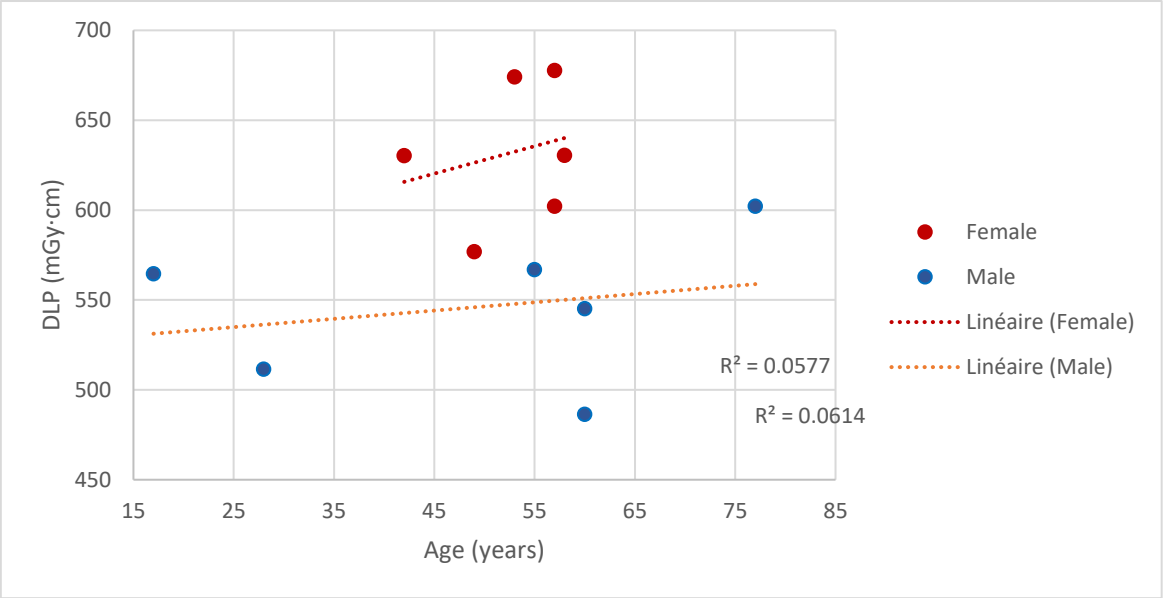


Figure III.2 : Relationship between Age and DLP According to Sex in Portal Venous Phase TAP CT Examinations

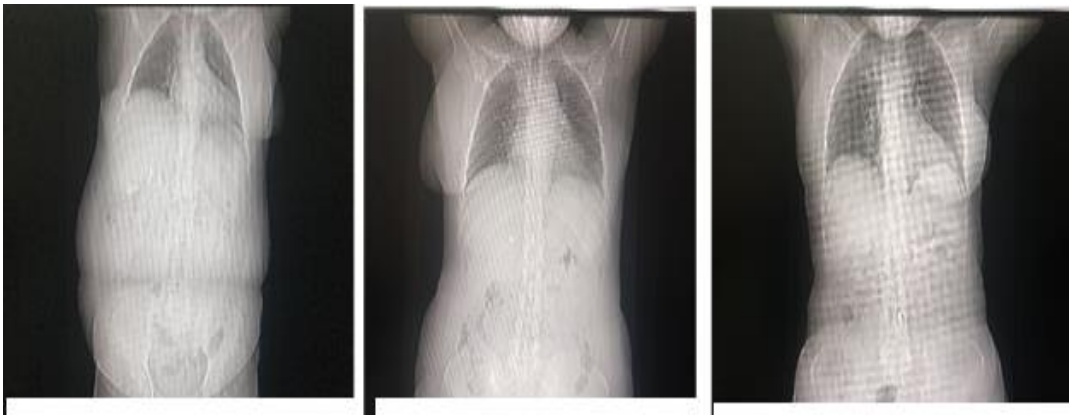


Figure III.3 : Scout images of patients 8, 12, and 7, respectively.

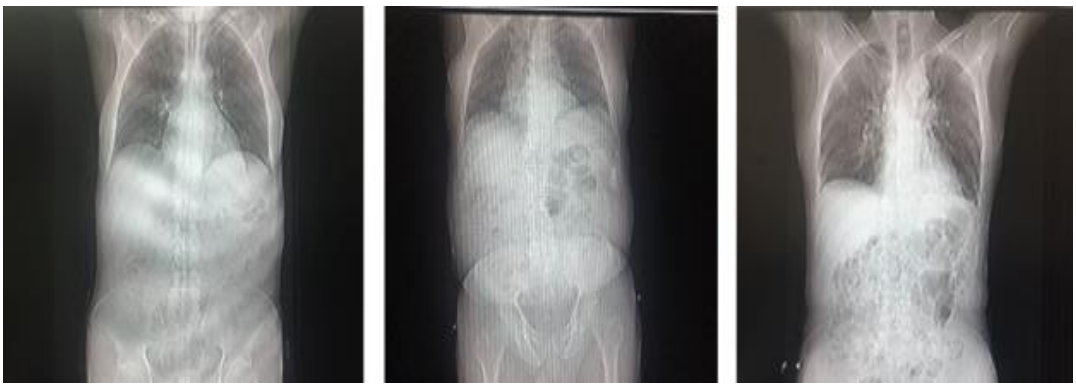


Figure III.4: Scout images of patients 1, 3, and 5, respectively.

The findings of the present study are consistent with those reported in study**[56] [57]**, **[58]**which indicated that the effect of sex on the radiation dose indices (CTDIvol and DLP) was

weak and not statistically significant. The study also found that age had no clear influence compared with the imaging protocol parameters. This was explained by the fact that automatic exposure control (AEC) systems primarily adjust the radiation output according to the patient's attenuation characteristics rather than demographic factors such as age or sex. Similarly, the results of the present study showed that the effects of both age and sex on CTDIvol and DLP values were limited. The correlation coefficients did not show a clear relationship between age and either dose index, and no significant differences were observed between males and females. These findings suggest that radiation dose in computed tomography is mainly determined by imaging protocol parameters, such as mAs, kVp, and automatic exposure control (AEC) systems, as well as patient-related factors, including body size and body mass index (BMI), rather than by age or sex.

2.2 Effect of mAs on Radiation Dose

Figure III.5 illustrates the relationship between tube current (mAs) and volumetric CT dose index (CTDIvol, mGy) during thoraco-abdomino-pelvic (TAP CT) examinations in the portal venous phase (liver), with a separation between males (blue) and females (red).

The results show that mAs values in males ranged from 81.9 to 112 mA·s, corresponding to CTDIvol values between 6.4 and 8.9 mGy. In females, mAs ranged from 94.9 to 112 mA·s, with CTDIvol values between 7.6 and 8.9 mGy. A clear overlap between both sexes is observed, particularly at higher dose levels within the upper range of CTDIvol values.

The findings indicate a strong near-linear positive relationship between mAs and CTDIvol in both groups, where radiation dose increases progressively with increasing mAs, with limited inter-patient variability. From a physical perspective, mAs is defined as the product of tube current (mA) and exposure time (s). Since the rotation time was constant (0.35 s), variations in mAs directly reflect changes in tube current. An increase in tube current leads to a higher number of electrons in the X-ray tube, resulting in increased photon production, a stronger radiation beam, and consequently a proportional increase in absorbed dose. In addition, automatic exposure control (AEC) adjusts tube current based on patient characteristics and attenuation in order to maintain image quality while minimizing radiation dose, which partly explains the limited variability observed between patients. The coefficient of determination confirms a strong linear correlation between the two variables in both sexes, with a slightly stronger correlation in females ($R^2 = 0.9879$) compared to males ($R^2 = 0.9135$).

Overall, the results demonstrate that mAs is one of the key technical factors influencing CTDIvol in TAP CT examinations, where increases in mAs lead to a direct increase in radiation

dose. Accordingly, optimal adjustment of this parameter within imaging protocols, together with the use of AEC, helps achieve a balance between image quality and radiation protection in line with the ALARA principle.

The findings of the present study are consistent with those reported in study[59][60] [61], which demonstrated a direct positive relationship between tube current (**mAs**) and radiation dose. An increase in **mAs** results in higher **CTDIvol** values because it increases the amount of X-rays produced during the examination. Similarly, the results of the present study showed a strong linear relationship between **mAs** and **CTDIvol** in both males and females, confirming that tube current is one of the most important technical factors influencing radiation dose in computed tomography.

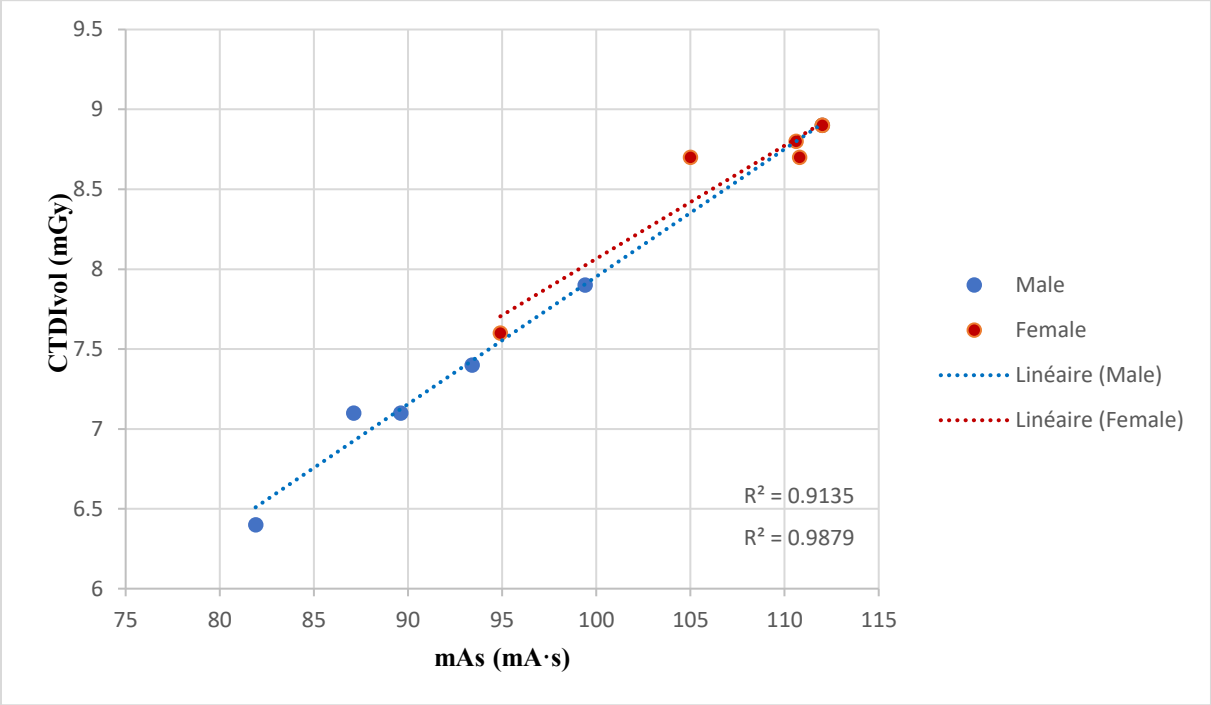


Figure III. 5 : Relationship Between mAs and CTDIvol According to Sex

3 Comparison of Radiation Dose According to Examination Type :

Table III.2 presents the radiation dose values CTDIvol and DLP for both TAP CT in the portal venous phase and Brain APC CT examinations. It includes the individual values for each patient, as well as the mean values for each examination. A clear and marked difference is observed between the two examination types for both dose metrics. The mean CTDIvol for TAP CT was 8.3 mGy, whereas for brain CT it reached 52.1 mGy, corresponding to approximately 6.3 times higher values. Similarly, the mean DLP for TAP CT was 598.65 mGy·cm, while for brain CT it was 1388.2 mGy·cm, about 2.3 times higher.

This difference in CTDIvol can be explained by the fact that brain CT protocols require higher exposure settings (kV and mAs) to achieve sufficient spatial resolution and contrast for evaluating sensitive brain structures. In addition, variations in imaging protocol and reconstruction techniques contribute to the increased dose levels in this type of examination. The difference in DLP is also influenced by scan length and the anatomical coverage specific to each examination figure III.6.

Overall, these results indicate that the type of examination is a major determinant of radiation dose levels, with Brain APC CT showing significantly higher doses compared to TAP CT. This highlights the importance of strict adherence to the ALARA principle when selecting and optimizing CT imaging protocol.

The results of this study are consistent with AAPM Report No. 96 [62] [63] [64] where the CTDIvol value for brain CT (52.1 mGy) is close to the reference levels reported for head examinations, while it remains lower in TAP CT (8.3 mGy), confirming that brain imaging generally requires higher radiation doses than body examinations. The difference in DLP between the two examinations also reflects the combined effect of radiation dose and scan length, as DLP is directly related to CTDIvol and the anatomical coverage of the scan, rather than dose alone.

Overall, these findings confirm that the type of examination and the imaging protocol are the primary factors determining radiation dose levels, in agreement with international recommendations and the ALARA principle

Table III.2 : Comparison of CTDIvol and DLP Values Between TAP CT (Portal Venous Phase) and Brain APC CT Examinations

Patient ID	Examination Type	CTDIvol (mGy)	DLP (mGy·cm)
P1	TAP CT – Portal Venous Phase (Liver)	7.9	567
P2	TAP CT – Portal Venous Phase (Liver)	8.7	630.3
Mean	TAP CT – Portal Venous Phase (Liver)	8.3	598.65
P3	Brain APC CT	56.5	1421.2
P4	Brain APC CT	47.7	1355.2
Mean	Brain APC CT	52.1	1388.2

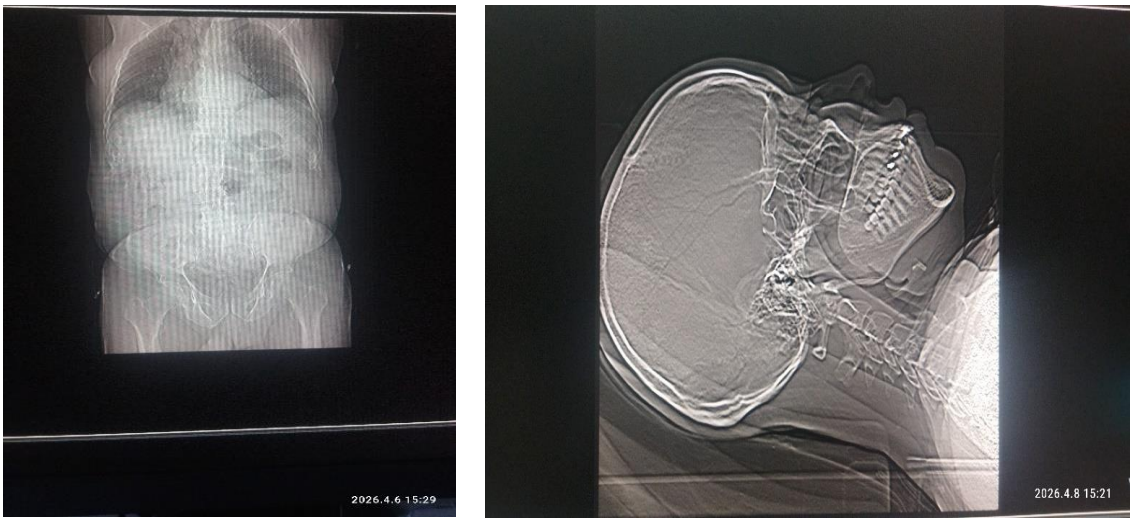


Figure III.6: Scout images of contrast-enhanced brain CT and TAP CT in the portal venous phase.

4 Image Quality Analysis

4.1 Noise Analysis

Table III.3 presents the measured image noise (Noise) values in patients during the studied CT examinations. The final noise value was calculated as the average of the two measured regions (Noise 1 and Noise 2). The noise values ranged from 10.83 to 18.39. The following section will examine the relationship between image noise and radiation dose.

Table III.3 : Patient image noise measurements during CT examinations

Patient Number	Sex	Age (years)	Noise 1	Noise 2	Noise
1	Male	28	11.47	11.688	11.579
2	Male	60	11.664	9.991	10.8275
3	Male	77	17.422	19.36	18.391
4	Male	17	12.303	12.205	12.254
5	Male	60	10.887	11.479	11.183
6	Male	55	13.121	12.764	12.9425
7	Female	49	13.095	11.911	12.503
8	Female	57	13.049	12.725	12.887
9	Female	58	17.654	16.082	16.868
10	Female	57	16.672	15.768	16.22
11	Female	53	15.248	15.58	15.414
12	Female	42	13.826	13.236	13.531

4.2 SNR Analysis

Table III.4 presents the measured signal-to-noise ratio (SNR) values in patients during the studied CT examinations. The SNR values were calculated based on the mean signal intensity (Mean 1 and Mean 2) and the corresponding noise levels in the two regions (Noise 1 and Noise 2). The SNR values ranged from 4.18 to 11.16. The following section will analyze the relationship between SNR and radiation dose.

Table III.4 : Patient SNR measurements during CT examinations

Patient Number	Sex	Age (years)	Mean 1	Noise 1	Mean 2	Noise 2	SNR 1	SNR 2	SNR
1	Male	28	128.023	11.47	122.184	11.688	11.16155187	10.45379877	10.80767532
2	Male	60	107.568	11.664	91.924	9.991	9.222222222	9.200680613	9.211451417
3	Male	77	107.359	17.422	104.836	19.36	6.1622661	5.415082645	5.788674372
4	Male	17	137.341	12.303	129.45	12.205	11.16321222	10.60630889	10.88476056
5	Male	60	113.428	10.887	109.51	11.479	10.41866446	9.540029619	9.979347041
6	Male	55	103.445	13.121	99.245	12.764	7.88392653	7.775383892	7.829655211
7	Female	49	139.509	13.095	130.5	11.911	10.65360825	10.95625892	10.80493358
8	Female	57	92	13.049	92.028	12.725	7.050348686	7.232062868	7.141205777
9	Female	58	88.657	17.654	89.238	16.082	5.021921378	5.548936699	5.285429039
10	Female	57	71.343	16.672	64.21	15.768	4.279210653	4.072171487	4.17569107
11	Female	53	101.75	15.248	98.759	15.58	6.673006296	6.338831836	6.505919066
12	Female	42	129.495	13.826	120.352	13.236	9.366049472	9.092777274	9.229413373

4.3 CNR Analysis

Table III.5 presents the measured contrast-to-noise ratio (CNR) values in patients during the studied CT examinations. The CNR values were calculated based on the difference in density between the two measurement regions (Mean 1 and Mean 2) relative to the recorded noise. The CNR values ranged from 0.002 to 1.445. The following section will examine the relationship between CNR and radiation dose.

Table III.5 : Patient CNR measurements during CT examinations

Patient Number	Sex	Age (years)	Mean 1	Mean 2	Contrast	Noise	CNR
1	Male	28	128.023	122.184	5.839	11.579	0.50427498
2	Male	60	107.568	91.924	15.644	10.8275	1.44483953
3	Male	77	107.359	104.836	2.523	18.391	0.13718667
4	Male	17	137.341	129.45	7.891	12.254	0.64395299
5	Male	60	113.428	109.51	3.918	11.183	0.35035321
6	Male	55	103.445	99.245	4.2	12.9425	0.32451227
7	Female	49	139.509	130.5	9.009	12.503	0.72054707
8	Female	57	92	92.028	0.028	12.887	0.00217273
9	Female	58	88.657	89.238	0.581	16.868	0.03444392
10	Female	57	71.343	64.21	7.133	16.22	0.43976572
11	Female	53	101.75	98.759	2.991	15.414	0.19404438
12	Female	42	129.495	120.352	9.143	13.531	0.67570763

5 Relationship Between Radiation Dose and Image Quality

Table III.6 presents the aggregated data derived from the previous results of the volumetric CT dose index (CTDIvol, mGy) and the image quality parameters, including image noise (Noise), signal-to-noise ratio (SNR), and contrast-to-noise ratio (CNR) in the included patients. These data were compiled in order to allow a graphical representation of the relationship between radiation dose and image quality metrics.

Table III.6 : CTDIvol and image quality metrics (Noise, SNR, CNR) in CT examinations

Patient Number	Sex	Age (years)	CTDIvol (mGy)	Noise	SNR	CNR
1	Male	28	7.1	11.579	10.80768	0.50427498
2	Male	60	6.4	10.8275	9.211451	1.44483953
3	Male	77	8.9	18.391	5.788674	0.13718667
4	Male	17	7.4	12.254	10.88476	0.64395299
5	Male	60	7.1	11.183	9.979347	0.35035321
6	Male	55	7.9	12.9425	7.829655	0.32451227
7	Female	49	7.6	12.503	10.80493	0.72054707
8	Female	57	8.9	12.887	7.141206	0.00217273
9	Female	58	8.7	16.868	5.285429	0.03444392
10	Female	57	8.9	16.22	4.175691	0.43976572
11	Female	53	8.8	15.414	6.505919	0.19404438
12	Female	42	8.7	13.531	9.229413	0.67570763

5.1 Relationship Between Dose and Noise

Figure III.7 illustrates the relationship between volumetric CT dose index (CTDIvol, mGy) and image noise (Noise) during thoraco-abdomino-pelvic (TAP CT) examinations, with a separation between males and females. Noise values ranged from 10.83 to 18.39 in males and from 12.50 to 16.87 in females, while CTDIvol values ranged from 6.4 to 8.9 mGy in both groups, without a clear linear relationship between the two variables.

The coefficients of determination show differences in the strength of the correlation between the two groups ($R^2 = 0.8769$ for males and $R^2 = 0.2639$ for females). This variation is mainly attributed to the narrower dose range in females compared with males, rather than a direct effect of sex.

Although an inverse physical relationship between dose and noise is expected, the results show variability due to the influence of automatic tube current modulation (ATCM), which adjusts dose according to patient attenuation. In addition, factors such as patient body habitus and image reconstruction parameters also affect noise levels.

Overall, the findings indicate that image noise does not depend on radiation dose alone, but results from the interaction of multiple technical and patient-related factors, highlighting the need to balance image quality with radiation dose reduction.

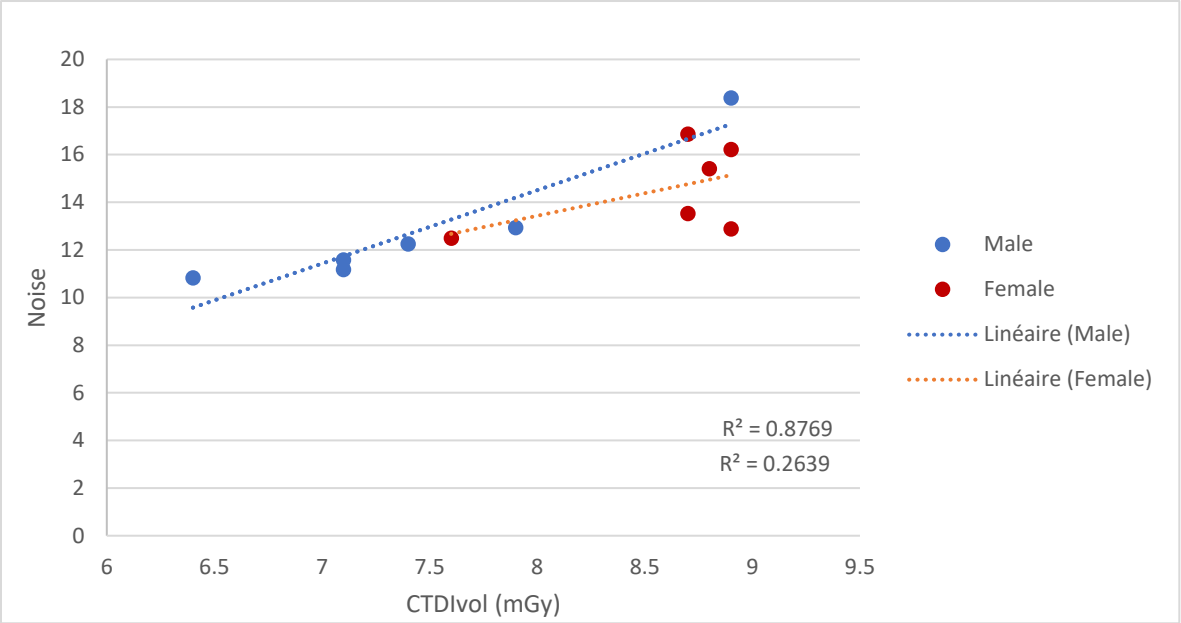


Figure III.7 : Relationship between CTDIvol and Noise during TAP CT examinations (portal venous phase)

5.2 Relationship Between Dose and SNR

Figure III.8 illustrates the relationship between volumetric CT dose index (CTDIvol, mGy) and signal-to-noise ratio (SNR) during thoraco-abdomino-pelvic (TAP CT) examinations in the portal venous phase of the liver, with a separation between male and female groups. SNR values ranged from 5.79 to 10.88 in males and from 4.18 to 10.80 in females, while CTDIvol ranged from 6.4 to 8.9 mGy in both groups. An overall inverse trend is observed between CTDIvol and SNR in both sexes, where SNR tends to decrease as dose increases. The highest SNR value (10.88) was recorded at a dose of 7.4 mGy in males, while the lowest value (4.18) was observed at 8.9 mGy in females.

The coefficients of determination ($R^2 = 0.5911$ for males and $R^2 = 0.5752$ for females) indicate a moderate inverse relationship between the two variables in both groups, with a close similarity in correlation strength. This behavior appears more consistent than that observed with image noise (Noise), suggesting that SNR more stably reflects dose-related variations despite the limited CTDIvol range in the study sample. The observed inverse trend can be indirectly explained by the effect of automatic tube current modulation (ATCM), which increases radiation dose in response to higher patient attenuation in individuals with larger body habitus. In parallel, increased tissue attenuation reduces the number of photons reaching the detector and increases image noise, which in turn leads to lower SNR values.

Therefore, the apparent inverse relationship between CTDIvol and SNR does not represent a direct causal link between dose and image quality, but rather reflects the influence

of patient size and tissue attenuation. ATCM adjusts the dose to compensate for attenuation, although it does not fully eliminate its impact on image quality.

Overall, the results indicate that SNR in CT imaging is not determined by radiation dose alone, but results from the interaction of multiple technical and biological factors. This highlights the need to balance radiation dose and image quality in accordance with the ALARA principle, ensuring adequate diagnostic quality at the lowest possible dose.

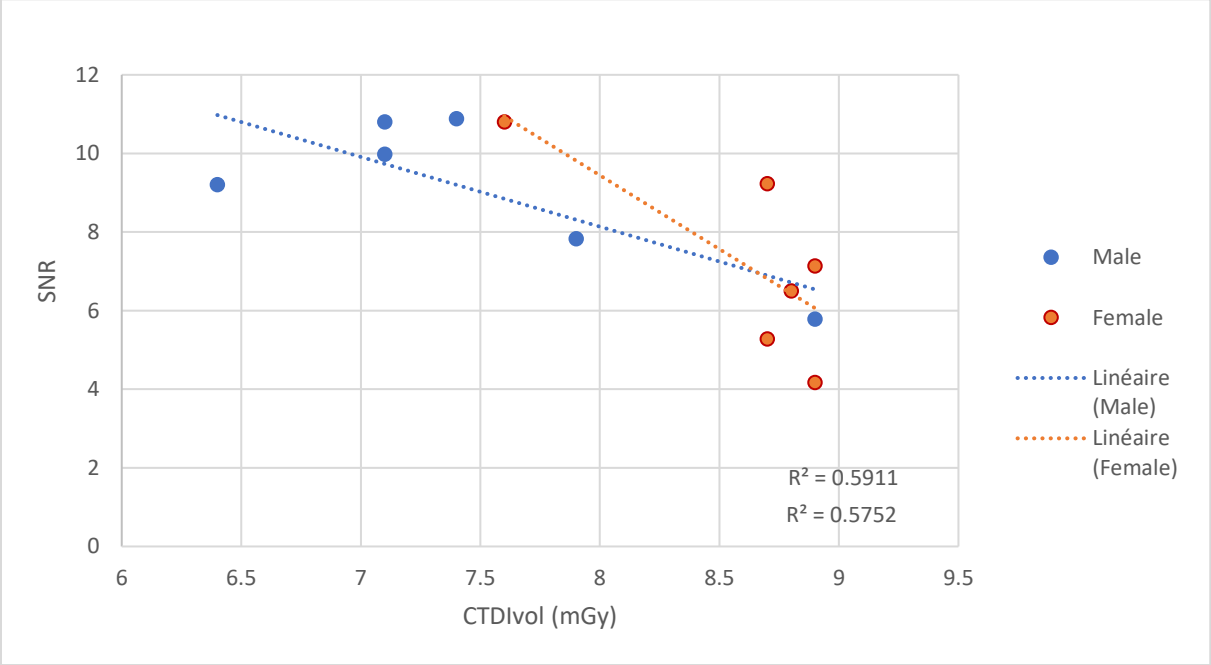


Figure III.8 : Relationship between CTDIvol and SNR during TAP CT examinations (portal venous phase)

5.3 Relationship Between Dose and CNR:

Figure III.9 illustrates the relationship between the volumetric CT dose index (CTDIvol, mGy) and the contrast-to-noise ratio (CNR) during thoraco-abdomino-pelvic (TAP CT) examinations, with a distinction between male and female groups.

CNR values ranged from 0.13 to 1.44 in males and from 0.00 to 0.72 in females, while CTDIvol ranged from 6.4 to 8.9 mGy in both groups. A variability in the CNR response to changes in dose is observed, without a clear linear trend, reflecting the indirect and complex nature of the relationship between the two variables in the studied sample. The coefficients of determination ($R^2 = 0.6222$ for males and $R^2 = 0.3716$ for females) indicate differences in the strength of the relationship between the two groups, being moderately strong in males and weaker in females. This difference is mainly attributed to the limited dose range within the sample, particularly in females, where the restricted variation in CTDIvol reduces the statistical

robustness of the model and affects the stability of the relationship, without indicating a direct effect of sex on contrast quality. Although the physical principle of CT imaging suggests improved contrast with increasing dose due to reduced noise, the results do not show a clear linear behavior. This can be explained by the influence of automatic tube current modulation (ATCM), which adjusts the dose according to patient attenuation in order to maintain image quality, making CTDIvol a dependent rather than fully independent variable. In addition, other factors contribute to this variability, such as patient anatomical characteristics, tissue attenuation distribution, and reconstruction parameters, all of which increase data dispersion and limit the linearity of the relationship between dose and CNR. Furthermore, calculating CNR between two regions within the same organ (liver) may reduce the dynamic range of values and affect the representation of true diagnostic contrast between different tissues.

Overall, the results confirm that CNR in CT imaging is not determined by radiation dose alone but results from the interaction of multiple technical and biological factors. This requires a balanced approach between optimizing image quality and reducing radiation dose in accordance with the ALARA principle.

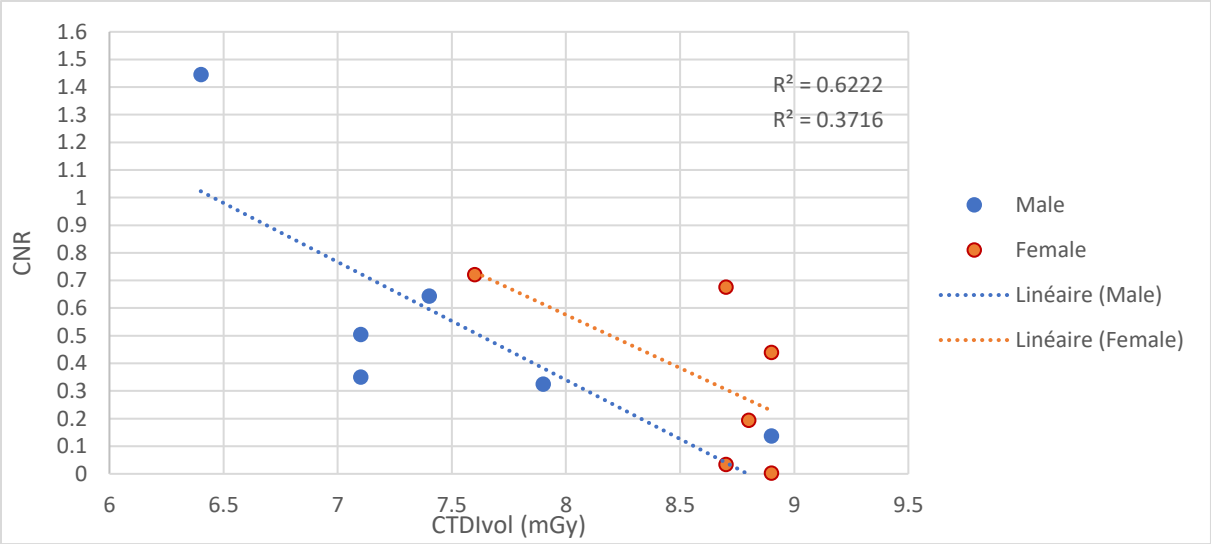


Figure III.9 : Relationship between CTDIvol and CNR during TAP CT examinations (portal venous phase)

5.3.1 Comparison with Previous Studies

The results of this study are consistent with those reported in Stud [65] [66] which demonstrated that the relationship between radiation dose (CTDIvol) and image quality metrics (CNR and SNR) is weak and non-linear, and that increasing dose does not consistently lead to a noticeable improvement in image quality. Similarly, the present study shows non-linear

relationships between CTDIvol and the image quality parameters Noise, SNR, and CNR, with variations in the strength of correlation between variables. This confirms that the effect of radiation dose on image quality is neither direct nor independent.

The reference study also highlighted significant variability between imaging systems and protocols, which helps explain the dispersion observed in the present results, particularly under the influence of automatic tube current modulation (ATCM), reconstruction techniques, and differences in patient characteristics.

Overall, both studies confirm that CT image quality does not depend on radiation dose alone, but is the result of a complex interaction between multiple technical and biological factors, thereby supporting the ALARA principle in optimizing the balance between dose and image quality.

6 Conclusion

The results of this chapter indicate that radiation dose in CT is primarily influenced by technical parameters, particularly tube current (mAs) and the standardized imaging protocol, rather than by patient age or sex. No clear relationship was observed between age and the radiation dose indicators (CTDIvol and DLP), and radiation dose values were generally comparable between male and female patients. A strong positive linear relationship was found between mAs and CTDIvol, confirming that tube current is the main parameter controlling radiation dose. Furthermore, contrast-enhanced brain CT examinations showed higher radiation dose levels than TAP CT examinations, reflecting differences in imaging protocols and clinical diagnostic requirements. The analysis also demonstrated that the relationship between radiation dose and image quality is not straightforward, as image noise, SNR, and CNR are affected by multiple factors, including automatic exposure control (AEC), patient attenuation, and image reconstruction parameters. Overall, these findings emphasize that optimizing CT examinations is not achieved by simply increasing radiation dose, but by maintaining an appropriate balance between diagnostic image quality and patient radiation exposure in accordance with the ALARA principle.

General Conclusion

This study investigated the relationship between radiation dose and image quality in contrast-enhanced thoraco-abdomino-pelvic computed tomography (TAP CT) performed during the portal venous phase. With the increasing use of CT in clinical practice, optimizing radiation dose while maintaining adequate diagnostic image quality has become a major concern in medical imaging. Therefore, this work was conducted in accordance with the ALARA (As Low As Reasonably Achievable) principle to contribute to dose optimization and patient radiation protection.

The main objective of this study was to evaluate the relationship between radiation dose and image quality in TAP CT examinations. More specifically, the study aimed to:

- assess the influence of demographic factors (age and sex) on radiation dose;
- investigate the effect of technical parameters, particularly tube current (mAs), on radiation dose indicators (CTDIvol and DLP);
- evaluate image quality using objective parameters (Noise, SNR, and CNR);
- compare radiation dose levels between TAP CT and contrast-enhanced brain CT examinations

The theoretical part of this work reviewed the principles of X-rays, computed tomography, radiation dosimetry, and image quality, together with the main technical and patient-related factors influencing these parameters. The practical part consisted of the analysis of CT examinations performed on twelve patients undergoing TAP CT during the portal venous phase. Radiation dose was assessed using CTDIvol and DLP, while image quality was evaluated using Noise, Signal-to-Noise Ratio (SNR), and Contrast-to-Noise Ratio (CNR)

The obtained results demonstrated that radiation dose was primarily influenced by technical parameters rather than demographic characteristics. No clear relationship was observed between age and radiation dose, and CTDIvol and DLP values were generally comparable between male and female patients. This finding reflects the use of a standardized acquisition protocol and the action of the Automatic Exposure Control (AEC) system, which adjusts the tube current according to patient attenuation while maintaining consistent image quality.

A strong positive relationship was observed between mAs and CTDIvol, confirming that tube current is the principal factor controlling radiation dose. Furthermore, comparison between TAP CT and contrast-enhanced brain CT demonstrated considerably higher radiation dose

levels in brain CT examinations because of differences in imaging protocols and diagnostic requirements.

Regarding image quality, the results showed that the relationship between radiation dose and image quality was not linear. Although increasing radiation dose may reduce image noise, image quality was also influenced by several additional factors, including patient characteristics, Automatic Exposure Control, and image reconstruction parameters. Consequently, patients receiving similar radiation doses did not always present identical image quality.

These findings are consistent with previous studies, which have demonstrated that image quality depends on the combined influence of multiple technical and anatomical factors rather than radiation dose alone.

Based on the obtained results, the hypothesis concerning the influence of technical parameters on radiation dose was confirmed, particularly the strong relationship between mAs and CTDIvol. However, the hypothesis proposing a direct linear relationship between radiation dose and image quality was only partially confirmed because image quality is affected by several interacting factors beyond radiation dose.

Accordingly, the main research question can be answered by stating that achieving an optimal balance between radiation dose and image quality does not depend simply on increasing radiation exposure. Instead, it requires appropriate protocol optimization together with the effective use of modern exposure control and image reconstruction technologies.

Despite the importance of these findings, several limitations should be acknowledged. The study included only twelve patients, limiting the statistical power and generalizability of the results. In addition, data were collected from a single CT scanner installed in one hospital. Body Mass Index (BMI), an important determinant of both radiation dose and image quality, was not available. Furthermore, image quality assessment was limited to a single anatomical region.

Based on the present findings, continued optimization of CT protocols is recommended to ensure the best possible balance between diagnostic image quality and radiation dose. Appropriate use of Automatic Exposure Control (AEC), periodic quality assurance and calibration of CT equipment, regular protocol review, and continuous staff training should remain priorities in radiology departments.

Particular attention should also be paid to radiation protection by ensuring proper justification of each CT examination, limiting the scanned region to the clinical area of interest,

selecting appropriate acquisition parameters according to patient characteristics, and maintaining adherence to the ALARA principle throughout clinical practice.

The establishment of national Diagnostic Reference Levels (DRLs) for CT examinations in Algeria would further contribute to harmonizing clinical practice and improving patient radiation safety.

Future research should include larger patient populations, multiple healthcare institutions, and different CT scanner models to improve the generalizability of the findings. Additional patient-related variables, particularly Body Mass Index (BMI), should be incorporated, together with advanced image reconstruction techniques and more comprehensive image quality metrics such as the Modulation Transfer Function (MTF) and Noise Power Spectrum (NPS).

In conclusion, this study demonstrates that radiation dose alone is not sufficient to determine image quality in computed tomography. Instead, image quality results from the interaction of several technical and patient-related factors, with tube current modulation playing a central role in dose optimization. These findings emphasize the importance of standardized imaging protocols, advanced dose management technologies, and continuous optimization strategies to ensure high diagnostic performance while minimizing radiation exposure. Ultimately, maintaining this balance remains essential for improving patient safety and ensuring compliance with the ALARA principle

References

[1] U. Busch, « Claims of priority – The scientific path to the discovery of X-rays », *Zeitschrift für Medizinische Physik*, vol. 33, nº 2, p. 230-242, mai 2023, doi: 10.1016/j.zemedi.2022.12.002.

[2] O. US EPA, « Radiation Basics ». Consulté le: 8 juin 2026. [En ligne]. Disponible sur: https://www.epa.gov/radiation/radiation-basics

[3] « Introduction to Radiological Physics and Radiation Dosimetry | Wiley Online Books ». Consulté le: 23 juin 2026. [En ligne]. Disponible sur: https://onlinelibrary.wiley.com/doi/book/10.1002/9783527617135

[4] *Radiation Biology: A Handbook for Teachers and Students*. Vienna: International Atomic Energy Agency (IAEA), 2010. [En ligne]. Disponible sur: https://www-pub.iaea.org/MTCD/Publications/PDF/TCS-42_web.pdf

[5] M. Berger, Q. Yang, et A. Maier, « X-ray Imaging », in *Medical Imaging Systems: An Introductory Guide*, A. Maier, S. Steidl, V. Christlein, et J. Hornegger, Éd., Cham (CH): Springer, 2018. Consulté le: 9 juin 2026. [En ligne]. Disponible sur: http://www.ncbi.nlm.nih.gov/books/NBK546155/

[6] M. Rehani, « Dose reduction in CT while maintaining diagnostic confidence: a feasibility/demonstration study », International Atomic Energy Agency, Vienna, Austria, 2009.

[7] « Ionizing radiation and health effects ». Consulté le: 8 juin 2026. [En ligne]. Disponible sur: https://www.who.int/news-room/fact-sheets/detail/ionizing-radiation-and-health-effects

[8] B. A. Houria, « EFFET DU TEMPS D'IRRADIATION BÉTA ET LA TEMPÉRATURE SUR LES PICS I-TL DU LiF(700). », Mémoire de Master, Université Saad Dahlab Blida 1, 2020.

[9] I. Aksnes, « History of X-rays - 125 years in the making (pt 2) », Excillum. Consulté le: 9 juin 2026. [En ligne]. Disponible sur: https://www.excillum.com/history-of-x-rays-x-ray-tubes/

[10] *Diagnostic Radiology Physics: A Handbook for Teachers and Students*.

[11] T. Brankova, « GoConqr - X- RAYS producing process », GoConqr. Consulté le: 9 juin 2026. [En ligne]. Disponible sur: https://www.goconqr.com/mindmap/3873113/x-rays-producing-process

[12] F. W. Aston, « Atoms and isotopes », juin 1924. doi: 10.1002/jctb.5000432306.

[13] M. Donya, M. Radford, A. ElGuindy, D. Firmin, et M. H. Yacoub, « Radiation in medicine: Origins, risks and aspirations », *Glob Cardiol Sci Pract*, vol. 2014, nº 4, p. 437-448, déc. 2014, doi: 10.5339/gcsp.2014.57.

[14] E. B. Podgorsak, *Radiation oncology physics: A handbook for teachers and students*. Vienna (Austria): Publisher IAEA, 2005.

[15] U. F. O. Themes, « Based on X-Rays », Radiology Key. Consulté le: 9 juin 2026. [En ligne]. Disponible sur: https://radiologykey.com/based-on-x-rays/

[16] « Pair Production, Radiation Types, Assignment Help ». Consulté le: 9 juin 2026. [En ligne]. Disponible sur: https://www.expertsmind.com/topic/radiation-types/pair-production-99281.aspx

[17] F. H. Attix, *INTRODUCTION TO RADIOLOGICAL PHYSICS AND RADIATION DOSIMETRY*. New York: John Wiley & Sons, 1986.

[18] J. D. Harrison *et al.*, « ICRP Publication 147: Use of Dose Quantities in Radiological Protection », *Ann ICRP*, vol. 50, nº 1, p. 9-82, févr. 2021, doi: 10.1177/0146645320911864.

[19] D. R. Fisher et F. H. Fahey, « APPROPRIATE USE OF EFFECTIVE DOSE IN RADIATION PROTECTION AND RISK ASSESSMENT », *Health Phys*, vol. 113, nº 2, p. 102-109, août 2017, doi: 10.1097/HP.0000000000000674.

[20] K. H. H. A. et Al, « Physics of X-Ray Production and Its Applications in Medicine », *Letters in High Energy Physics*, vol. 2023, nº Issue 2, févr. 2023, Consulté le: 8 juin 2026. [En ligne]. Disponible sur: https://www.lettersinhighenergyphysics.com/index.php/LHEP/article/view/934

[21] « Normal Chest X-Ray ». Consulté le: 23 juin 2026. [En ligne]. Disponible sur: https://amismedical.com/normal-chest-x-ray/

[22] « SELENIA HOLOGIC DIGITAL MAMMOGRAPHY WITH FLAT PANEL DETECTOR FROM 2009 AND X-RAY TUBE FROM 2014 in Montreuil, Île-de-France, France ». Consulté le: 23 juin 2026. [En ligne]. Disponible sur: https://www.machinio.com/listings/85087467-selenia-hologic-digital-mammography-with-flat-panel-detector-from-2009-and-x-ray-tube-from-2014-in-montreuil-france

[23] « Une personne allongée sur un lit photo – Image gratuite de Médical sur Unsplash ». Consulté le: 23 juin 2026. [En ligne]. Disponible sur: https://unsplash.com/fr/photos/une-personne-allongee-sur-un-lit-ibdJjGbrgxI

[24] International Commission on Radiological Protection (ICRP), « The 2007 Recommendations of the ICRP (ICRP Publication 103) », Publication 103, 2007.

[25] G. Paulo *et al.*, « Diagnostic Reference Levels based on clinical indications in computed tomography: a literature review », *Insights Imaging*, vol. 11, nº 1, p. 96, août 2020, doi: 10.1186/s13244-020-00899-y.

[26] Y. A. Al-Naser et D. Tafti, « CT Instrumentation and Physics », in *StatPearls*, Treasure Island (FL): StatPearls Publishing, 2026. Consulté le: 15 juin 2026. [En ligne]. Disponible sur: http://www.ncbi.nlm.nih.gov/books/NBK597347/

[27] S. Hermena et M. Young, « CT-scan Image Production Procedures », in *StatPearls*, Treasure Island (FL): StatPearls Publishing, 2026. Consulté le: 15 juin 2026. [En ligne]. Disponible sur: http://www.ncbi.nlm.nih.gov/books/NBK574548/

[28] J. Cobos Alonso, C. Fontenla-Martínez, L. Concepción Aramendía, J. M. Bernabé García, et J. J. Arenas-Jiménez, « Introduction to iodinated contrasts: Properties, intravenous administration and distribution throughout the body », *Radiología (English Edition)*, vol. 66, p. S3-S14, oct. 2024, doi: 10.1016/j.rxeng.2024.03.010.

[29] W. Brisbane, M. R. Bailey, et M. D. Sorensen, « An overview of kidney stone imaging techniques », *Nat Rev Urol*, vol. 13, nº 11, p. 654-662, nov. 2016, doi: 10.1038/nrurol.2016.154.

[30] K. J. Fowler *et al.*, « Universal Liver Imaging Lexicon: Imaging Atlas for Research and Clinical Practice », *RadioGraphics*, vol. 43, nº 1, p. e220066, janv. 2023, doi: 10.1148/rg.220066.

[31] Y. Inoue, « Radiation Dose Management in Computed Tomography: Introduction to the Practice at a Single Facility », *Tomography*, vol. 9, nº 3, p. 955-966, mai 2023, doi: 10.3390/tomography9030078.

[32] F. R. Verdun *et al.*, « Image quality in CT: From physical measurements to model observers », *Physica Medica*, vol. 31, nº 8, p. 823-843, déc. 2015, doi: 10.1016/j.ejmp.2015.08.007.

[33] « Spatial Resolution - an overview | ScienceDirect Topics ». Consulté le: 15 juin 2026. [En ligne]. Disponible sur: https://www.sciencedirect.com/topics/earth-and-planetary-sciences/spatial-resolution

[34] M. T. Niknejad, « Contrast resolution | Radiology Reference Article | Radiopaedia.org », Radiopaedia. Consulté le: 15 juin 2026. [En ligne]. Disponible sur: https://radiopaedia.org/articles/contrast-resolution

[35] G. T. Herman, « On the noise in images produced by computed tomography », *Computer Graphics and Image Processing*, vol. 12, nº 3, p. 271-285, mars 1980, doi: 10.1016/0146-664X(80)90015-5.
[36] D. J. Bell, « Radiological image artifact | Radiology Reference Article | Radiopaedia.org », Radiopaedia. Consulté le: 15 juin 2026. [En ligne]. Disponible sur: https://radiopaedia.org/articles/radiological-image-artifact
[37] Á. Rodríguez Sánchez, A. Thompson, L. Körner, N. Brierley, et R. Leach, « Review of the influence of noise in X-ray computed tomography measurement uncertainty », *Precision Engineering*, vol. 66, août 2020, doi: 10.1016/j.precisioneng.2020.08.004.
[38] Á. Rodríguez Sánchez, A. Thompson, L. Körner, N. Brierley, et R. Leach, « Review of the influence of noise in X-ray computed tomography measurement uncertainty », *Precision Engineering*, vol. 66, août 2020, doi: 10.1016/j.precisioneng.2020.08.004.
[39] « Modulation Transfer Function - an overview | ScienceDirect Topics ». Consulté le: 15 juin 2026. [En ligne]. Disponible sur: https://www.sciencedirect.com/topics/medicine-and-dentistry/modulation-transfer-function.com
[40] « Noise Power Spectrum - an overview | ScienceDirect Topics ». Consulté le: 15 juin 2026. [En ligne]. Disponible sur: https://www.sciencedirect.com/topics/computer-science/noise-power-spectrum.com
[41] M. Donoghue, B. Tuohy, N. Colgan, D. Lavin, et W. van der Putten, « Development and implementation of a DQE technique to assess image quality for digital radiology systems in the Saolta University Healthcare Group », *Physica Medica*, vol. 32, nº 7, p. 959, juill. 2016, doi: 10.1016/j.ejmp.2016.05.050.
[42] H. R. Mendes, J. C. Silva, M. Marcondes, et A. Tomal, « Optimization of image quality and dose in adult and pediatric chest radiography via Monte Carlo simulation and experimental methods », *Radiation Physics and Chemistry*, vol. 201, p. 110396, nov. 2022, doi: 10.1016/j.radphyschem.2022.110396.
[43] S. P. Raman, M. Mahesh, R. V. Blasko, et E. K. Fishman, « CT Scan Parameters and Radiation Dose: Practical Advice for Radiologists », *Journal of the American College of Radiology*, vol. 10, nº 11, p. 840-846, nov. 2013, doi: 10.1016/j.jacr.2013.05.032.
[44] A. Goel, « Kilovoltage peak | Radiology Reference Article | Radiopaedia.org », Radiopaedia. Consulté le: 15 juin 2026. [En ligne]. Disponible sur: https://radiopaedia.org/articles/kilovoltage-peak
[45] « Impact of Patient Size and Positioning on Radiation Dose in Multiphase Liver CT Examinations ». Consulté le: 15 juin 2026. [En ligne]. Disponible sur: https://www.mdpi.com/2076-3417/15/11/5815.com
[46] Y. Gao *et al.*, « A comparison of pediatric and adult CT organ dose estimation methods », *BMC Med Imaging*, vol. 17, nº 1, p. 28, avr. 2017, doi: 10.1186/s12880-017-0199-3.
[47] E. Angel *et al.*, « Dose to Radiosensitive Organs During Routine Chest CT: Effects of Tube Current Modulation », *AJR Am J Roentgenol*, vol. 193, nº 5, p. 1340-1345, nov. 2009, doi: 10.2214/AJR.09.2886.
[48] A. E. Papadakis et J. Damilakis, « Evaluation of an organ-based tube current modulation tool in pediatric CT examinations », *Eur Radiol*, vol. 30, nº 10, p. 5728-5737, oct. 2020, doi: 10.1007/s00330-020-06888-5.
[49] B. Kataria, J. N. Althén, Ö. Smedby, A. Persson, H. Sökjer, et M. Sandborg, « Assessment of image quality in abdominal CT: potential dose reduction with model-based iterative reconstruction », *Eur Radiol*, vol. 28, nº 6, p. 2464-2473, juin 2018, doi: 10.1007/s00330-017-5113-4.

[50] G. R. Iball et D. S. Brettle, « Organ and effective dose reduction in adult chest CT using abdominal lead shielding », *Br J Radiol*, vol. 84, nº 1007, p. 1020-1026, nov. 2011, doi: 10.1259/bjr/53865832.

[51] M. Bani-Ahmad, Y. H. Hadi, A. O. Sullivan, A. England, L. McLaughlin, et M. McEntee, « Clinical indication–based CT scan range reduction: A scoping review of radiation dose savings and diagnostic accuracy », *Journal of Medical Imaging and Radiation Sciences*, vol. 57, nº 3, p. 102338, mai 2026, doi: 10.1016/j.jmir.2026.102338.

[52] S. L. Cohen, T. J. Ward, A. Makhnevich, S. Richardson, et M. D. Cham, « Retrospective analysis of 1118 outpatient chest CT scans to determine factors associated with excess scan length », *Clin Imaging*, vol. 62, p. 76-80, juin 2020, doi: 10.1016/j.clinimag.2019.11.020.

[53] H. W. Goo, « CT Radiation Dose Optimization and Estimation: an Update for Radiologists », *Korean J Radiol*, vol. 13, nº 1, p. 1-11, 2012, doi: 10.3348/kjr.2012.13.1.1.

[54] « Process ». Consulté le: 15 juin 2026. [En ligne]. Disponible sur: http://www.iaea.org/resources/hhc/medical-physics/radiology/process

[55] L. W. Goldman, « Principles of CT: Radiation Dose and Image Quality », *Journal of Nuclear Medicine Technology*, vol. 35, nº 4, p. 213-225, déc. 2007, doi: 10.2967/jnmt.106.037846.

[56] P. Prakash, M. K. Kalra, M. D. Gilman, J.-A. O. Shepard, et S. R. Digumarthy, « Is weight-based adjustment of automatic exposure control necessary for the reduction of chest CT radiation dose? », *Korean J Radiol*, vol. 11, nº 1, p. 46-53, 2010, doi: 10.3348/kjr.2010.11.1.46.

[57] Z. Y. Hamd *et al.*, « AI-Driven Prediction of Chest CT Radiation Doses: Establishing BMI-Based Diagnostic Reference Levels and Patient–Factor Correlations for Machine-Learning Models », *Tomography*, vol. 12, nº 5, p. 61, mai 2026, doi: 10.3390/tomography12050061.

[58] Y. Inoue, H. Itoh, K. Nagahara, H. Hata, et K. Mitsui, « Relationships of Radiation Dose Indices with Body Size Indices in Adult Body Computed Tomography », *Tomography*, vol. 9, nº 4, p. 1381-1392, juill. 2023, doi: 10.3390/tomography9040110.

[59] S. Elojeimy, S. Tipnis, et W. Huda, « Relationship between radiographic techniques (kilovolt and milliampere-second) and CTDI(VOL) », *Radiat Prot Dosimetry*, vol. 141, nº 1, p. 43-49, sept. 2010, doi: 10.1093/rpd/ncq138.

[60] A. Zhao, S. Fopma, et R. Agrawal, « Demystifying the CT Radiation Dose Sheet », *RadioGraphics*, vol. 42, nº 4, p. 1239-1250, juill. 2022, doi: 10.1148/rg.210107.

[61] « Relationships between Size-specific Dose Estimate and Signal to Noise Ratio under Chest CT Examinations with Tube Current Modulation », *Current Medical Imaging*, vol. 20, janv. 2024, doi: 10.2174/0115734056267251231121064259.

[62] « AAPM Report No 96-5.qxd ». Consulté le: 15 juin 2026. [En ligne]. Disponible sur: https://www.aapm.org/pubs/reports/RPT_96.pdf.com

[63] E. Atlı, S. A. Uyanık, U. Öğüşlü, H. Çevik Cenkeri, B. Yılmaz, et B. Gümüş, « Radiation doses from head, neck, chest and abdominal CT examinations: an institutional dose report », *Diagn Interv Radiol*, vol. 27, nº 1, p. 147-151, janv. 2021, doi: 10.5152/dir.2020.19560.

[64] I. Garba, F. Zarb, M. F. McEntee, et S. G. Fabri, « Computed tomography diagnostic reference levels for adult brain, chest and abdominal examinations: A systematic review », *Radiography (Lond)*, vol. 27, nº 2, p. 673-681, mai 2021, doi: 10.1016/j.radi.2020.08.011.

[65] L. A. G. Røhme *et al.*, « Image quality and radiation doses in abdominal CT: A multicenter study », *Eur J Radiol*, vol. 178, p. 111642, sept. 2024, doi: 10.1016/j.ejrad.2024.111642.

[66] M. J. Willemink et P. B. Noël, « The evolution of image reconstruction for CT—from filtered back projection to artificial intelligence », *Eur Radiol*, vol. 29, nº 5, p. 2185-2195, mai 2019, doi: 10.1007/s00330-018-5810-7.

الجمهورية الجزائرية الديمقراطية الشعبية
République Algérienne Démocratique et Populaire
وزارة التعليم العالي و البحث العلمي
Ministère de l'Enseignement Supérieur et de la Recherche

Université 20 août 1955-Skikda

جامعة 20 اوت 1955- سكيكدة

Faculté des Sciences

كلية العلوم

Département de Physique

قسم الفيزياء

سكيكدة يوم: 2026/04/....

رقم: ... و ف 2026

محضر تصحيح مذكرة الماستر

أنا الممضي أسفله الأستاذ(ة) المشرف(ة): بن زروق حيان

أشهد بأن الطالب (ة): سطوطاح يسرى

تخصص: فيزياء طبية

قد قام(ت) بجميع التصحيحات المتعلقة بمذكرة الماستر

تحت عنوان: Study of the relation ship between radiation dose and image quality in computed Tomography (CT)

امضاء الأستاذ(ة) المشرف(ة)

رئيس القسم